The Plant Cell, Vol. 31: 734–751, March 2019, www.plantcell.org © 2019 ASPB.

AMP and GMP Catabolism in Arabidopsis Converge on Xanthosine, Which Is Degraded by a Nucleoside Hydrolase Heterocomplex

Chiara Baccolini and Claus-Peter Witte[1]

Department of Molecular Nutrition and Biochemistry of Plants, Institute of Plant Nutrition, Leibniz University Hannover, Herrenhäuser Straße 2, 30419 Hannover, Germany

ORCID IDs: 0000-0002-0517-0100 (C.B.); 0000-0002-3617-7807 (C.-P.W.)

Plants can fully catabolize purine nucleotides. A firmly established central intermediate is the purine base xanthine. In the current widely accepted model of plant purine nucleotide catabolism, xanthine can be generated in various ways involving either inosine and hypoxanthine or guanosine and xanthosine as intermediates. In a comprehensive mutant analysis involving single and multiple mutants of urate oxidase, xanthine dehydrogenase, nucleoside hydrolases, guanosine deaminase, and hypoxanthine guanine phosphoribosyltransferase, we demonstrate that purine nucleotide catabolism in Arabidopsis (*Arabidopsis thaliana*) mainly generates xanthosine, but not inosine and hypoxanthine, and that xanthosine is derived from guanosine deamination and a second source, likely xanthosine monophosphate dephosphorylation. Nucleoside hydrolase 1 (NSH1) is known to be essential for xanthosine hydrolysis, but the in vivo function of a second cytosolic nucleoside hydrolase, NSH2, is unclear. We demonstrate that NSH1 activates NSH2 in vitro and in vivo, forming a complex with almost two orders of magnitude higher catalytic efficiency for xanthosine hydrolysis than observed for NSH1 alone. Remarkably, an inactive NSH1 point mutant can activate NSH2 in vivo, fully preventing purine nucleoside accumulation in *nsh1* background. Our data lead to an altered model of purine nucleotide catabolism that includes an NSH heterocomplex as a central component.

INTRODUCTION

Plants can synthesize purine and pyrimidine nucleotides and use salvage reactions to recycle nucleosides and nucleobases into the nucleotide pool (Stasolla et al., 2003; Zrenner et al., 2006). Unlike most animals, plants are also capable of full nucleotide catabolism, releasing the ring nitrogen (Zrenner et al., 2009; Werner and Witte, 2011) for reassimilation into amino acids. In the current model of purine nucleotide catabolism, a branched network of reactions beginning at 5′AMP and 5′GMP leads to the generation of the purine base xanthine as first common intermediate of all branches (Figure 1; see, e.g., Zrenner et al., 2006; Kopecná et al., 2013; Ashihara et al., 2018). The subsequent oxidation and hydrolysis of the xanthine ring via uric acid into glyoxylate, CO_2, and NH_4^+ occur in a linear sequence of reactions (Werner and Witte, 2011), as fully described in the last decade (Todd and Polacco, 2006; Werner et al., 2008, 2010, 2013; Lamberto et al., 2010; Pessoa et al., 2010; Serventi et al., 2010). If this pathway is interrupted by mutation of urate oxidase (*UOX*) in Arabidopsis (*Arabidopsis thaliana*), toxic amounts of uric acid accumulate and interfere with peroxisome maintenance in the embryo and cause severe defects in germination and seedling establishment (Hauck et al., 2014).

The model of a branched reaction network leading to xanthine from the mononucleotides has been derived from a multitude of studies (Schubert and Boland, 1990), mostly using radiolabeled metabolites added to plant extracts (Atkins, 1981; Shelp and Atkins, 1983), plant tissue preparations, or cell cultures (Ashihara et al., 1997; Katahira and Ashihara, 2006; Deng and Ashihara, 2010; Yin et al., 2014) and tracing the metabolic distribution of the label. Plant cells readily take up nucleobases and nucleosides, but not nucleotides, limiting the choice for radiotracer studies with intact tissues or cells to the nonphosphorylated nucleotide metabolism intermediates. To assess whether the enzymes for the postulated metabolic conversions occur in vivo, enzymatic activities in cell-free preparations were sometimes determined as well (Triplett et al., 1980; Shelp and Atkins, 1983; Atkins et al., 1989; Katahira and Ashihara, 2006).

In recent years, genes encoding some of these enzymes have been identified. Mutants of nucleoside hydrolase 1 (*NSH1*; formerly uridine hydrolase 1, *URH1*) of Arabidopsis were shown to accumulate high amounts of xanthosine as well as uridine (Jung et al., 2009; Riegler et al., 2011), demonstrating that this enzyme has a role in purine and pyrimidine nucleoside catabolism. After 5 d of darkness, inosine concentrations were also slightly elevated in the *NSH1* mutant compared to the the wild-type control (Jung et al., 2011), consistent with the current model showing either inosine or xanthosine as alternative intermediates of AMP and GMP catabolism (Figure 1). An Arabidopsis mutant of guanosine deaminase (*GSDA*) described by Dahncke and Witte (2013) accumulated high amounts of guanosine genetically demonstrating that plants catabolize G (guanylates, guanosine, guanine) on the level of guanosine as previously postulated based on radiotracer experiments (Ashihara et al., 1997). By contrast, animals and

[1] Address correspondence to cpwitte@pflern.uni-hannover.de.
The author responsible for distribution of materials integral to the findings presented in this article in accordance with the policy described in the Instructions for Authors (www.plantcell.org) is: Claus-Peter Witte (cpwitte@pflern.uni-hannover.de).
www.plantcell.org/cgi/doi/10.1105/tpc.18.00899

IN A NUTSHELL

Background: Nitrogen is a key element for plant growth and is constantly recycled in plant metabolism, for example, by the breakdown of the nitrogen-containing bases in nucleic acids. The current model of AMP and GMP degradation proposes a branched network of reactions, either involving inosine and hypoxanthine or alternatively xanthosine as intermediates to reach the nucleobase xanthine, which is the established entry point for the reactions that release nitrogen from the purine ring. A central enzyme for both branches is nucleoside hydrolase 1 (NSH1), which hydrolyzes both inosine and xanthosine. NSH1 is also required in pyrimidine nucleotide degradation for the hydrolysis of uridine. Apart from NSH1, plants possess a conserved second nucleoside hydrolase, NSH2, of unclear function.

Question: Is the current model of purine nucleotide breakdown correct? Are the inosine and xanthosine routes both employed for the degradation of AMP and GMP? Is NSH2 involved in purine nucleotide degradation and what is its role?

Findings: Quantifying metabolites by mass spectrometry in a series of Arabidopsis mutants and double mutants of genes involved in purine nucleotide degradation, we show that AMP and GMP are mainly degraded via xanthosine, whereas the route via inosine is not used. However, inosine and hypoxanthine were always present in small amounts, probably derived from other sources, such as vacuolar t-RNA breakdown or DNA repair. By biochemical analysis, we show that NSH2 forms a complex with NSH1 and is activated by this interaction. The NSH1/NSH2 complex is a highly efficient xanthosine (and inosine) hydrolase, whereas NSH1 alone is a more efficient uridine hydrolase. We conclude that Arabidopsis and probably many other plants degrade AMP and GMP via xanthosine as intermediate employing an NSH1/NSH2 complex for xanthosine hydrolysis.

Next steps: Which are the enzymatic steps leading to the production of xanthosine from AMP and GMP, in particular which are the phosphatases involved? How is the entry into purine nucleotide degradation regulated, and how is the AMP degradation route functionally separated from the biosynthetic route of GMP, since both routes share common intermediates?

microbes employ guanine deaminases for the deamination of G and its catabolism (Fernández et al., 2009). In an *NSH1 GSDA* double mutant, xanthosine could no longer be detected, leading to the notion that most, if not all, xanthosine is derived from guanosine and not from xanthosine monophosphate (XMP; Dahncke and Witte, 2013). However, an earlier study using cell-free extracts of cowpea (*Vigna unguiculata*) root nodules suggested that XMP rather than GMP is a precursor of purine nucleotide breakdown products (Atkins, 1981), which would imply the existence of an XMP phosphatase (XMPP). Plant genes encoding the putative phosphatases and kinases that metabolically link the nucleotides IMP (inosine monophosphate), XMP, and GMP with the nucleosides inosine, xanthosine, and guanosine in vivo have not been discovered. However, it has been firmly established that especially guanosine and to a lesser extent also inosine, but not xanthosine, can be salvaged into nucleotides and nucleic acids when these nucleosides are administered to plant tissue preparations or cell cultures. This suggests that plants possess an inosine guanosine kinase (IGK) but lack a xanthosine kinase. If nucleosides are not salvaged, they are degraded (Katahira and Ashihara, 2006; Deng and Ashihara, 2010; Yin et al., 2014; Ashihara et al., 2018). Nucleobases can be salvaged as well. Phosphoribosyltransferases replace the pyrophosphate in 5-phosphoribosly-1-pyrophosphate with the nucleobase generating mononucleotides. The gene for a plant hypoxanthine guanine phosphoribosyltransferase (*HGPRT*) has been cloned and the enzyme characterized. HGPRT has a sixfold lower K_m value for guanine compared with hypoxanthine (Liu et al., 2007). It has recently been shown that an *HGPRT* mutant accumulates guanine (Schroeder et al., 2018), genetically demonstrating that HGPRT actually operates as a guanine phosphoribosyltransferase in vivo. Whether HGPRT also salvages hypoxanthine in vivo is unknown. Similar to guanosine and inosine, guanine and hypoxanthine can be salvaged when administered to plant cells or tissues, but the salvage of guanine is more efficient, whereas hypoxanthine is mostly catabolized. By contrast, xanthine is not salvaged at all (Katahira and Ashihara, 2006; Deng and Ashihara, 2010; Yin et al., 2014; Ashihara et al., 2018).

NSH2, a close homolog to NSH1, is conserved in plants (Kopecná et al., 2013) and is thought to be involved in cytosolic purine nucleoside catabolism. In tissue extracts of Arabidopsis *NSH2* mutants, xanthosine and inosine, but not uridine, hydrolytic activity was reduced (Riegler et al., 2011). However, neither xanthosine nor inosine accumulated in plants lacking *NSH2* (Jung et al., 2011; Riegler et al., 2011). When *NSH2* was strongly overexpressed (>60-fold compared to the the wild type), some, but not all lines showed a two- to threefold increased inosine hydrolase activity in the extract (Jung et al., 2011). Biochemical analysis of NSH2 from vascular plants was hampered by the marked insolubility of the recombinant protein (Jung et al., 2011; Riegler et al., 2011; Kopecná et al., 2013), but an NSH2 homolog from the moss *Physcomitrella patens* could be obtained as soluble dimeric protein showing strong inosine and xanthosine hydrolase activity and weak activity with adenosine and guanosine (Kopecná et al., 2013). Interestingly, the recombinant NSH1 homolog of *Physcomitrella* is highly insoluble, whereas NSH1 from vascular plants is a soluble protein readily amenable to biochemical analysis. In summary, these data indicate that NSH2 of vascular plants might be involved in purine nucleoside catabolism, but its role in vivo remains obscure, and it cannot be positioned correctly in the current model (Figure 1).

In this work, a range of single, double, and triple null mutants of genes encoding enzymes involved in purine nucleotide catabolism and salvage of Arabidopsis were generated, and alterations in phenotypes and corresponding metabolite profiles were recorded

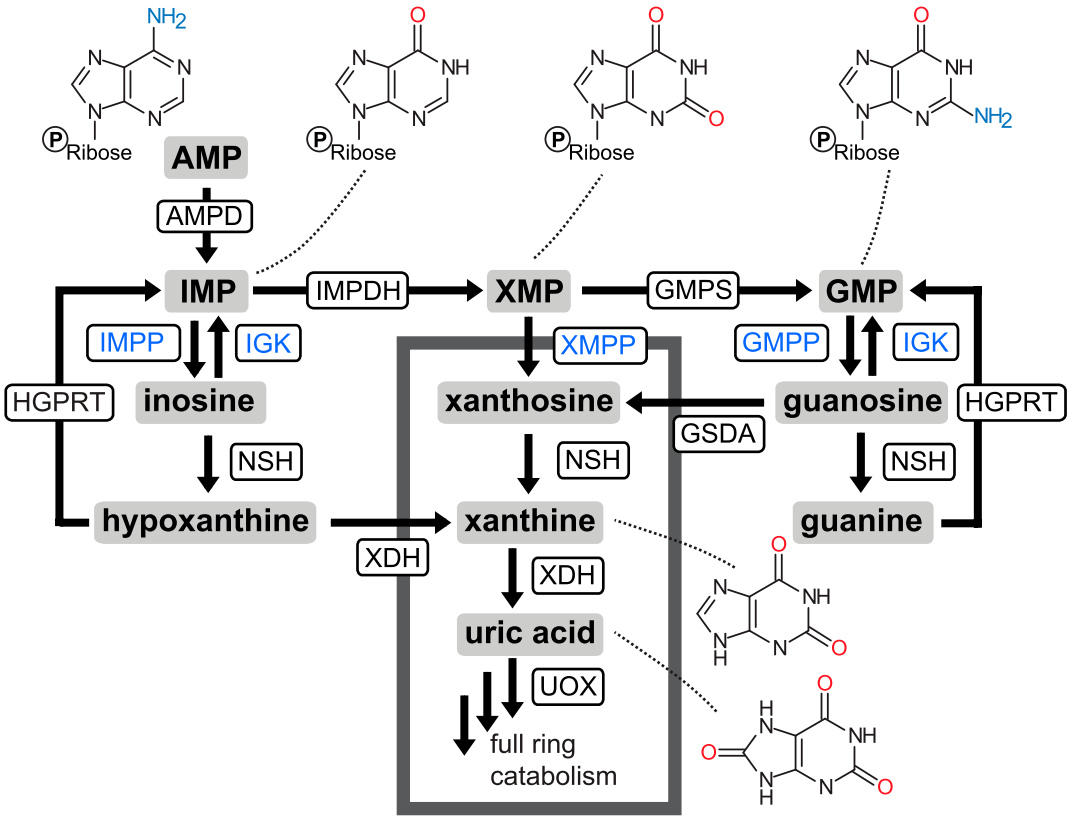

Figure 1. Current Model of Purine Nucleotide Catabolism in Arabidopsis.

The figure was redrawn from Yin et al. (2014) and slightly simplified. Similar models of the pathway can be found in Riegler et al. (2011) or in reviews (Stasolla et al., 2003; Zrenner et al., 2006). Metabolites: IMP, inosine monophosphate; XMP, xanthosine monophosphate. Enzymes: AMPD, AMP deaminase; IMPDH, IMP dehydrogenase; GMPS, GMP synthetase; HGPRT, hypoxanthine guanine phosphoribosyltrnasferase; IMPP, IMP phosphatase; XMPP, XMP phosphatase; GMPP, GMP phosphatase (IMPP, XMPP, and GMPP are usually summarized as 5′-nucleotide phosphatase not specifying whether the enzyme[s] are nucleotide specific); IGK, inosine guanosine kinase; GSDA, guanosine deaminase; NSH, nucleoside hydrolase; XDH, xanthine dehydrogenase; UOX, urate oxidase (uricase). Enzyme names are shown in blue if the corresponding enzyme is presumed to be involved but the genetic identity is unclear. The gray box encloses metabolites that can only be catabolized, but not salvaged. Note that the conversion of nucleotides and nucleosides can also be catalyzed by phosphotransferases (data not shown) transferring phosphate from a donor mononucleotide onto an acceptor nucleoside. However, such reactions will not create changes in the total nucleoside/mononucleotide pool sizes; therefore, no net salvage or degradation will occur. Oxo- and amino-substituents on the purine ring are highlighted in red and blue, respectively.

to elucidate the catabolic pathway of purine nucleotides used in vivo. The integration of these data with the current knowledge led to a modified, more linear model of plant purine nucleotide catabolism. Additionally, we obtained genetic as well as biochemical evidence that NSH2 is an intrinsic component of purine nucleotide catabolism. NSH2 absolutely requires interaction with NSH1 for activation. Our data demonstrate that in vivo purine nucleoside hydrolysis is catalyzed by an NSH1-NSH2 complex and not by NSH1 alone.

RESULTS

Genetic Suppression of the *UOX* Mutant

A *UOX* mutant of Arabidopsis accumulates uric acid in all tissues. The particularly high concentration in embryos compromises peroxisome maintenance in this tissue, with drastic consequences for germination and seedling establishment. Many seeds do not germinate, and those that do are usually unable to establish a seedling, unless Suc is supplied from outside (Hauck et al., 2014). This phenotype can be suppressed by crossing the *UOX* mutant with a mutant of xanthine dehydrogenase (*XDH*). Because XDH lies metabolically upstream of UOX (Figure 1), the double mutant accumulates xanthine instead of uric acid, which has no obvious deleterious effects to the plant. Consequently, it must be the uric acid and not the lack of UOX or the defective purine catabolism per se that causes the strong phenotypes in *uox* (Hauck et al., 2014).

To elucidate whether a gene is involved in purine catabolism upstream of *UOX*, a mutant allele of the gene in question can be crossed into the *uox* background, assessing the potential suppression of the *uox* phenotypes and of uric acid accumulation in the double mutant. We have generated double mutants of *uox* with

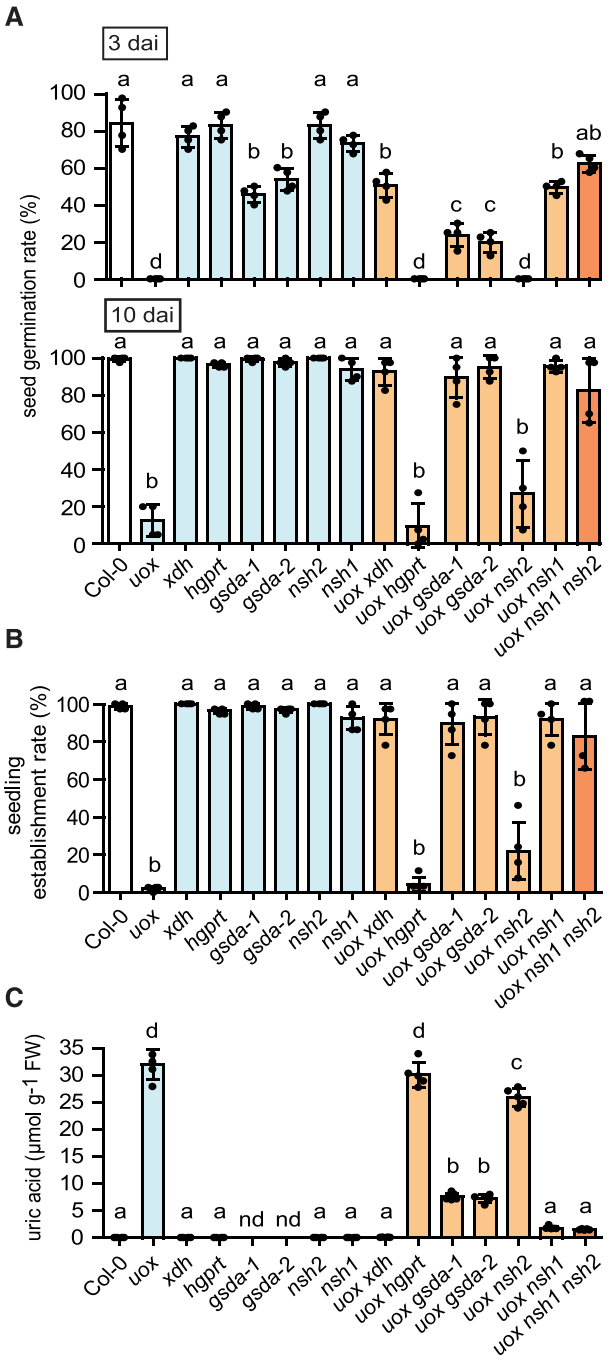

Figure 2. Genetic Suppression of the *UOX* Mutant Phenotypes.

Several genotypes were analyzed: the wild type (Col-0, white bars) and single mutants (blue bars) of *UOX*, *XDH*, *HGPRT*, *GSDA* (*GSDA-1*, *GSDA-2*), *NSH2*, and *NSH1* as well as double mutants (light orange bars) and triple mutants (dark orange bars) in the *uox* background. Individual data points (dots) of biological replicates and the mean (bar) are shown. Biological replicates were generated from seeds of different individuals grown side by side. Error bars are SD. The statistical analyses were performed using one-way ANOVA with Tukey's post test. Different letters indicate significant differences ($P < 0.05$). nd, not detectable. FW, fresh weight.

xdh, *hgprt*, *nsh1*, and *nsh2* and two alleles of *gsda*, *gsda-1* and *gsda-2*, as well as the triple mutant *uox nsh1 nsh2*. All of these mutant alleles have been previously described and represent functional knockouts of the respective genes. Neither the *uox* phenotypes in germination (Figure 2A; Supplemental Figure 1A) and seedling establishment (Figure 2B; Supplemental Figure 1B) nor the uric acid accumulation in seeds (Figure 2C) was altered in *uox hgprt* background. In human, where purine catabolism naturally ends with uric acid as the final product, a defect of *HGPRT* causes uric acid hyperaccumulation, leading to severe phenotypic consequences called the Lesch–Nyhan syndrome. Here, defective guanine and/or hypoxanthine salvage boosts purine nucleobase catabolism. This is apparently not the case in Arabidopsis seeds, because defective *HGPRT* in the *uox* background does not lead to further increased uric acid accumulation. The data indicate that neither guanine nor hypoxanthine is an intermediate of purine nucleotide catabolism in Arabidopsis, which has been suggested already for guanine (Dahncke and Witte, 2013), but not for hypoxanthine.

The strongest suppression of the *uox* phenotypes and the uric acid accumulation was observed in the *uox xdh* genotype, corroborating results from Hauck et al. (2014). The data confirm that a second *XDH*-like gene found in the Arabidopsis genome (*XDH2*, At4g34900) is not relevant for the generation of uric acid and that it therefore does not contribute to purine nucleotide catabolism in this plant.

Suppression in the *uox nsh1* background was strong as well, abolishing almost all uric acid accumulation in seeds and thereby demonstrating that NSH1 has a central function for cytosolic purine nucleoside hydrolysis. Interestingly, also in the *uox nsh2* line a slightly diminished uric acid accumulation was observed in seeds, and the *uox* phenotypes seemed less severe, indicating that also NSH2 is involved in purine nucleoside catabolism. However, an additive suppressive effect of *NSH1* and *NSH2* abrogation in the *uox* background was not observed.

Both *uox gsda* double-mutant lines showed strong suppression of the *uox* phenotypes. Note that mutation of *GSDA* alone was previously found to delay seed germination (Schroeder et al., 2018), as could be confirmed here (Figure 2A). Uric acid accumulation was strongly, but not completely, prevented in seeds of the *uox gsda* double-mutant lines, indicating that purine nucleotide catabolism depends to a great extent, yet not fully, on the GSDA reaction. The GSDA-independent flow through the pathway might pass through a putative XMPP or through the IMP-inosine-hypoxanthine branch according to the current model (Figure 1).

Purine Nucleoside and Nucleobase Accumulation in Seeds and Seedlings of Mutants in Purine Catabolism

Similar to uric acid accumulation in seeds of the *uox* background, xanthine accumulation in seeds as well as in seedlings of the *xdh*

(A) Germination rate at 3 and 10 d after imbibition (dai; $n = 4$ biological replicates).
(B) Seedling establishment rate. Percentage of seedlings established 15 d after sowing ($n = 4$ biological replicates).
(C) Uric acid content in seeds ($n = 5$ biological replicates).

background is (1) not altered by mutation of *HGPRT* (*xdh hgprt* line); (2) strongly suppressed in an *XDH NSH1* mutant; (3) weakly but significantly suppressed in an *xdh nsh2* line; and (4) strongly, but not completely, suppressed in an *XDH GSDA* mutant (Figures 3A and 3B, top left). This independent data set confirms that HGPRT does not seem to have a marked influence on purine catabolism, whereas NSH1 and GSDA play major roles and NSH2 is also important. Again, the results show that the GSDA reaction is partially bypassed either through an XMPP or through an IMPP giving access to the inosine-hypoxanthine branch (Figure 1). The data in Figures 2C and 3 indicate that the flux through the bypass is quantitatively smaller than the flux through GSDA.

How is GSDA bypassed? If there was a significant flux through the inosine-hypoxanthine branch, one would expect accumulation of inosine and hypoxanthine in mutants that block this branch. Interestingly, the *XDH* mutant does not accumulate hypoxanthine (Figure 3), which has also been noted by Brychkova et al. (2008), although xanthine and hypoxanthine are both substrates of XDH (Figure 1). In accordance, blocking XDH activity chemically with allopurinol in soybean (*Glycine max*) and tobacco (*Nicotiana tabacum*) resulted only in xanthine, but not in hypoxanthine, accumulation (Fujihara and Yamaguchi, 1978; Boland and Schubert, 1982; Montalbini and DellaTorre, 1995). However, in cowpea nodules, 5% to 10% hypoxanthine with reference to xanthine was detected upon allopurinol treatment (Atkins et al., 1988). Although the general lack of hypoxanthine accumulation in plant tissues without active XDH suggests that hypoxanthine is not an intermediate of purine nucleotide catabolism, hypoxanthine could potentially be salvaged by HGPRT, preventing its accumulation, whereas xanthine is not salvaged (Ashihara et al., 2018). In the *xdh hgprt* background, where salvage is also blocked, we indeed observed some hypoxanthine accumulation in seeds and seedlings, but the hypoxanthine concentration was always at least one order of magnitude smaller than the xanthine concentration (Figure 3). In seeds, hypoxanthine even accumulated in an *xdh gsda* background, where high guanosine and in consequence guanine levels were reached. Guanine is the preferred substrate of HGPRT (Liu et al., 2007), probably limiting the enzyme's availability for hypoxanthine and leading to its accumulation. As shown above (Figures 2 and 3), *HGPRT* abrogation in the *uox* or *xdh* background does not boost the concentration of the purine nucleotide catabolites uric acid or xanthine, in contrast to what is observed in human. These results together with the comparatively small accumulation of hypoxanthine in the *xdh hgprt* background suggest that hypoxanthine is not a major intermediate of purine nucleotide catabolism in Arabidopsis.

Similarly, the amount of inosine accumulating in the *NSH1* mutant was >400 times lower than the amount of xanthosine in seeds and seedlings (Figure 3). However, as hypoxanthine, inosine can be salvaged to some extent according to radiotracer experiments (Ashihara et al., 2018), presumably by a dual-specific IGK (Combes et al., 1989) which has not yet been identified genetically. Salvage might reduce inosine accumulation in the *nsh1* background, whereas xanthosine cannot be salvaged (Ashihara et al., 2018). Our data indicate that a dual-specific IGK is also present in Arabidopsis, because upon strong guanosine accumulation in the *gsda* background of seeds (*gsda* and *xdh gsda* lines; Figure 3A) an elevated inosine concentration is consistently observed (Figure 3A), possibly because IGK is fully occupied with guanosine in this situation and therefore not available for inosine. We examined whether the inosine concentration would strongly increase in the *nsh1* background, where degradation is blocked, if salvage is also compromised by high guanosine amounts — a situation occurring in *nsh1 gsda* seeds. However, we observed only a slightly higher inosine concentration in *nsh1 gsda* seeds versus *nsh1* seeds (Figure 4A), indicating that inosine salvage does not play an important role. Therefore, even when salvage is likely compromised, the inosine concentration in seeds remains approximately two orders of magnitude smaller than the concentration of xanthosine in the *nsh1* background (Figure 4A). This is also the case in seedlings and the rosette of 4-week-old plants (Figures 4B and 4C). It appears that inosine, similar to hypoxanthine, is not a major intermediate of purine nucleotide catabolism in vivo. Hence, the flux through AMP/GMP catabolism that bypasses GSDA is not routed through an IMPP to access the inosine-hypoxanthine branch but runs probably through an XMPP which generates xanthosine. This concept is strongly supported by the observation that xanthosine accumulation in the *nsh1* background is not completely suppressed in seeds and seedlings when *GSDA* is additionally abrogated (Figures 4A and 4B). The xanthosine remaining in the *nsh1 gsda* background is very likely generated by the XMPP. Consistently, uric acid and xanthine accumulation in seeds and seedlings of *uox* and *xdh* backgrounds, respectively, is highly, but never fully, suppressed by *GSDA* abrogation (Figures 2 and 3). In rosette leaves of 4-week-old plants, a stronger suppression of xanthosine accumulation in the *nsh1 gsda* background is observed than in seeds and seedlings (Figure 4C), indicating that here GSDA dominates xanthosine generation with hardly any contribution from XMPP. This is mirrored by a stronger suppression of xanthine accumulation in *xdh gsda* double mutants in that tissue (Supplemental Figure 2).

Taken together, our data suggest that AMP and GMP degradation in Arabidopsis are both routed through xanthosine and not inosine in vivo. It is likely that inosine and hypoxanthine are derived from other sources. Inosine occurs in transfer RNA (tRNA), and there are six nuclear tRNAs containing inosine in Arabidopsis (Zhou et al., 2014). Upon vacuolar degradation of tRNA, inosine will be released into the cytosol, probably via the equilibrative nucleoside exporter 1 (Bernard et al., 2011). Hypoxanthine accumulates to ~10-fold higher concentrations than inosine in seeds and seedlings in the respective mutants (Figure 3), indicating that it is not only derived from the hydrolysis of inosine. Hypoxanthine may stem from base excision repair of DNA. It occurs in DNA due to erroneous incorporation of deoxyinosine triphosphate by DNA polymerases and because adenine spontaneously deaminates to hypoxanthine at a low rate (Alseth et al., 2014). Similarly, the usual origin of guanine in plant metabolism might be spontaneous depurination of nucleotides and nucleic acids (An et al., 2014). Hence, the physiological role of HGPRT is to salvage hypoxanthine and guanine from these sources, whereas purine nucleotide catabolism generates xanthine without a hypoxanthine or guanine intermediate and is thereby decoupled from HGPRT activity in Arabidopsis. By contrast, such decoupling is not observed in human, where HGPRT counteracts excessive purine base catabolism, preventing uric acid accumulation and the development of the Lesch–Nyhan syndrome.

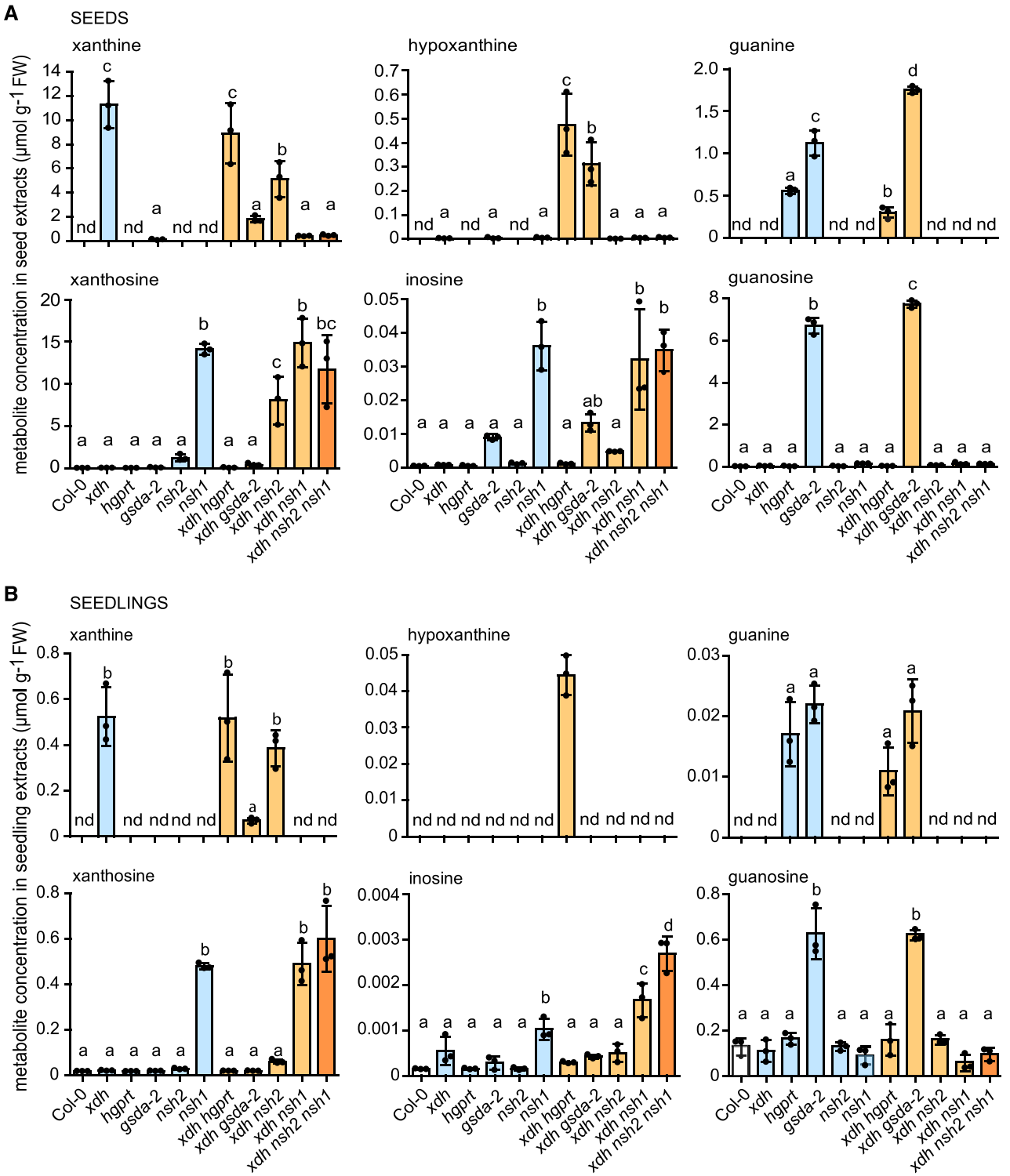

Figure 3. Purine Nucleobase and Nucleoside Content in Seeds and Seedlings of the Wild Type, Several Mutants of Genes Involved in Purine Nucleotide Catabolism and Salvage, and Double as Well as Triple Mutants in the *xdh* Background.

Individual data points (dots) of biological replicates and the mean (bar) are shown. Three biological replicates generated from seeds of different individuals grown side by side were analyzed per genotype and tissue. Error bars are SD. The statistical analyses were performed using one-way ANOVA with Tukey's post test. Different letters indicate significant differences ($P < 0.05$). nd, not detectable. FW, fresh weight.

(A) Seeds.

(B) Ten-day-old seedlings.

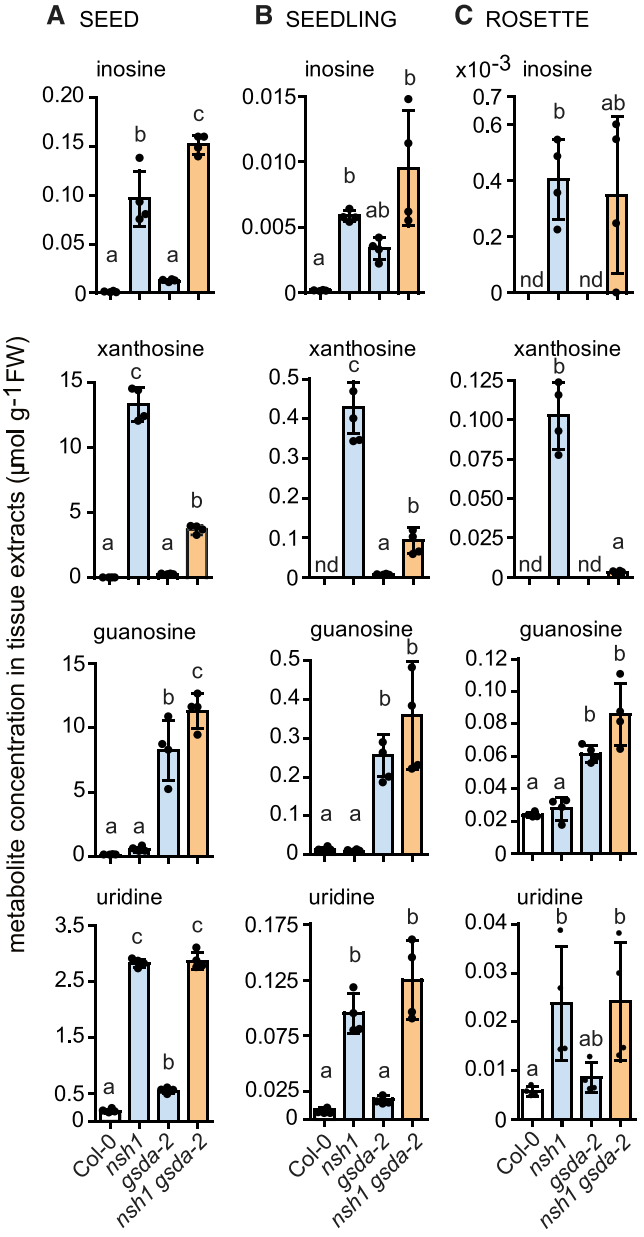

Figure 4. Nucleoside Content in Seeds, Seedlings, and Rosettes of *NSH1 GSDA* Double Mutants and the Respective Single Mutants as Well as the Wild Type.

Individual data points (dots) of biological replicates and the mean (bar) are shown. Four biological replicates generated from seeds of different individuals grown side by side were analyzed per genotype and tissue. Error bars are SD. The statistical analyses were performed using one-way ANOVA with Tukey's post test. Different letters indicate significant differences ($P < 0.05$). nd, not detectable. FW, fresh weight.

(A) Seeds.

(B) Seven-day-old seedlings.

(C) Rosettes of 4-week-old plants just before bolting.

The Role of NSH2

There are several indications for a function of NSH2 in purine nucleotide catabolism from our mutant analyses. (1) The accumulation of uric acid in seeds and the resulting macroscopic phenotypes during germination and seedling establishment of the *UOX* mutant are partially suppressed in a *UOX NSH2* double mutant (Figure 2; Supplemental Figure 1). (2) An *XDH NSH2* mutant also accumulates less xanthine than the *XDH* mutant in seeds (Figure 3A), a tendency that is also observed in seedlings (Figure 3B). (3) The xanthosine concentration appears elevated in *NSH2* mutant seeds without reaching statistical significance (Figure 3A), but (4) strikingly, xanthosine accumulates strongly in seeds of the *XDH NSH2* double mutant (Figure 3A). However, it is known that NSH1, but not NSH2, is essential to prevent high accumulation of xanthosine in vivo (Figure 3; Jung et al., 2011; Riegler et al., 2011). It is possible that the high concentration of xanthine in the *xdh* background causes product inhibition of NSH1, reducing the efficiency of xanthosine catabolism, which only becomes apparent if additionally, *NSH2* is absent. Is NSH2 an activator of NSH1? Or is NSH2 itself a xanthosine hydrolase that is activated by NSH1? In both scenarios, NSH1 and NSH2 might physically interact.

NSH2 Is a Xanthosine and Inosine Hydrolase That Strictly Requires NSH1 for Activity

A detailed enzymatic characterization of purified NSH2 from vascular plants has been hampered mainly by the low solubility of the enzyme when it was expressed in *Escherichia coli* (Jung et al., 2011; Riegler et al., 2011; Kopecná et al., 2013). Here, we transiently expressed N-terminally Strep-tagged variants of NSH1 and NSH2 in leaves of *Nicotiana benthamiana* and were able to obtain highly pure and soluble enzymes after affinity purification (Figure 5). The NSH1 preparation was active with xanthosine and uridine, confirming previous findings (Jung et al., 2009; Riegler et al., 2011). By contrast, purified NSH2 showed no hydrolytic activity with these substrates (Table 1).

The results of our mutant analyses indicated that NSH1 and NSH2 might physically interact. This notion was experimentally tested by coexpressing N-terminally Strep- and myc-tagged variants of NSH1 and NSH2 in *N. benthamiana* leaves and assessing whether the myc-tagged variants could be copurified upon affinity purification of the respective Strep-tagged enzymes. We found that NSH1 and NSH2 indeed interact, because myc-tagged NSH1 can be copurified with Strep-tagged NSH2 and vice versa (Figure 6). Interestingly, NSH1 also interacts with itself, whereas NSH2 does not. The lack of activity of NSH2 and its inability to form homomers is surprising, because the NSH2 homolog from the moss *P. patens* was shown to have xanthosine and inosine hydrolase activity and to form dimers (Kopecná et al., 2013).

Specific polyclonal antibodies against NSH1 and NSH2 were developed to assess by immunoprecipitation (IP) experiments whether the untagged native proteins interact in Arabidopsis. Unfortunately, we were unable to obtain an antibody for NSH2 that did not also cross-react with NSH1, even after multiple rounds of affinity purification of the antibody preparation. However,

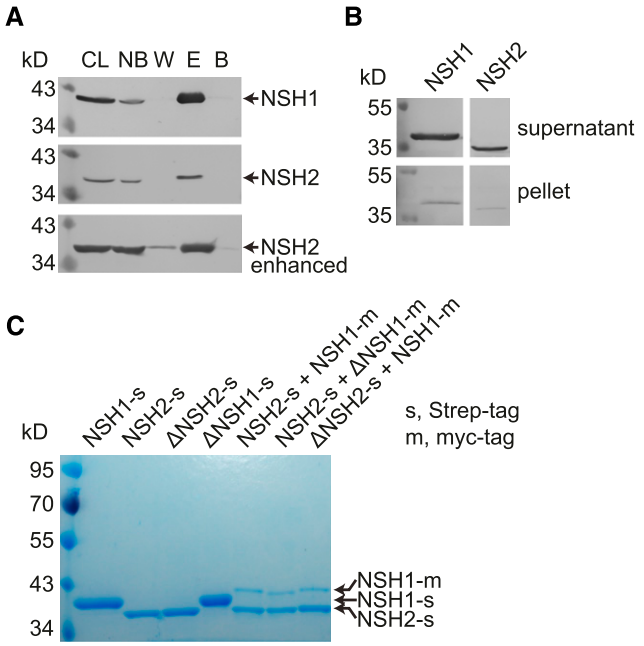

Figure 5. Purification of Nucleoside Hydrolases with Strep Affinity Chromatography.

(A) Purification of N-terminally Strep-tagged NSH1 and NSH2 transiently expressed in *N. benthamiana* leaves (top and middle panels, respectively). To boost expression of NSH2, an additional construct containing viral enhancer sequences (see "Methods") was used (bottom panel). Proteins were detected by immunoblot with StrepTactin-alkaline phosphatase conjugate. CL, clarified cell lysate; NB, protein not bound to the affinity matrix; W, protein in the last washing step; E, elution fraction; B, protein remaining bound to the affinity matrix after elution.

(B) Solubility of transiently expressed NSH1 and NSH2. Clarified cell lysates of *N. benthamiana* leaves expressing either NSH1 or NSH2 were centrifuged at 100,000*g* for 1 h. The supernatant and the pellet fractions were analyzed on an immunoblot using StrepTactin-alkaline phosphatase detection.

(C) Purity of affinity (co)purified nucleoside hydrolases. SDS gel loaded with 12.5 μL of the affinity-purified enzymes (elution fraction) that either had been expressed alone as Strep-tagged variants or together with myc-tagged variants. ΔNSH1 and ΔNSH2 are inactive point mutants of NSH1 and NSH2. The gel was stained with colloidal Coomassie blue.

a difference in electrophoretic mobility of both enzymes allowed them to be distinguished on immunoblots. The dual-specific anti-NSH1/2 antibody was used to detect both enzymes after the IP performed with the mono-specific anti-NSH1 antibody. The IP experiments using root extracts of hydroponically grown wild-type, *nsh1*, and *nsh2* plants demonstrated that native NSH1 and NSH2 interact with each other in Arabidopsis (Figure 7).

The expression of NSH1 and NSH2 was assessed with immunoblots using the anti-NSH1 antibody as well as the dual-specific NSH1/2 antibodies in seedlings, roots, and the rosettes of plants before bolting, and in different tissues of flowering plants (Figure 8). The blots were loaded with extracts obtained from an equal fresh weight of tissue. With both antibodies, NSH1 was detected in all tissues, showing that NSH1 is a ubiquitously expressed enzyme. By contrast, NSH2 could only be detected

Table 1. Specific Activities of NSH Enzymes, Enzyme Complexes, and Variants

Specific Activity (μmol min^{-1} mg^{-1})				
NSH[a]		Xanthosine (0.25 mM)	Inosine (0.25 mM)	Uridine (0.25 mM)
1	-[b]	0.61 ± 0.01	0[c]	5.7 ± 0.2
-	2	0	0	0
1	2	15.4 ± 0.4	3.9 ± 0.9	2.0 ± 0.5
Δ1	-	0	0	0
Δ1	2	6 ± 2	0[c]	0[c]
-	Δ2	0	0	0
1	Δ2	0.22 ± 0.02	0	0.4 ± 0.1

Errors are SD (n = 3).

[a]NSH1-NSH2 heterocomplexes were always purified via Strep-tagged NSH2 to avoid excess NSH1.

[b]-indicates that only one nucleoside hydrolase was expressed and purified.

[c]Activities were detected at higher substrate concentrations (see Supplemental Table 1).

clearly in roots, seedlings, and flowers, although the dual-specific antibody is as sensitive for NSH2 as for NSH1 (Supplemental Figure 3).

In roots, NSH2 often appears only slightly less abundant than NSH1 (Figures 7 and 8B; Supplemental Figure 3). In several other tissues, NSH2 is not sufficiently abundant to be clearly detected in our immunoblots, although public transcriptome data show that NSH2 transcript is ubiquitously present. Crystal structure and size exclusion chromatography data showed that plant NSH proteins form dimers (Kopecná et al., 2013). The higher abundance of NSH1 compared with NSH2 indicates that in vivo a homodimeric NSH1 complex and a heterodimeric NSH1-NSH2 complex will usually be present.

Because of the higher abundance of NSH2 in roots, we investigated whether the abrogation of NSH2 has a marked impact

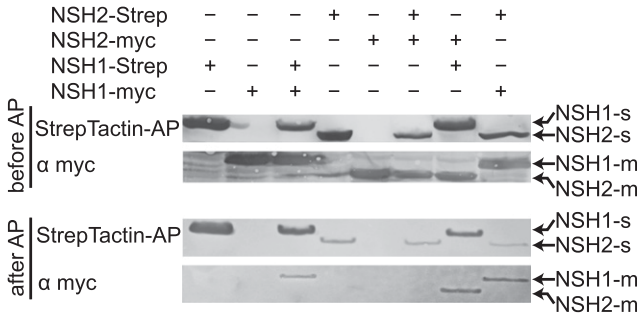

Figure 6. Interaction of NSH1 and NSH2 In Planta.

NSH1 and NSH2 were transiently coexpressed as Strep- or myc-tagged variants in *N. benthamiana* leaves in the combinations indicated. Affinity purification was performed using the Strep tag. Protein expression (top) and protein (co)purification by affinity chromatography (bottom) were assessed on immunoblots developed with either StrepTactin-AP conjugate or anti-myc antibodies. Per lane, 12 μL of clarified leaf extracts or affinity-purified proteins were loaded. AP, affinity purification; suffix -m, myc-tagged; suffix -s, Strep-tagged.

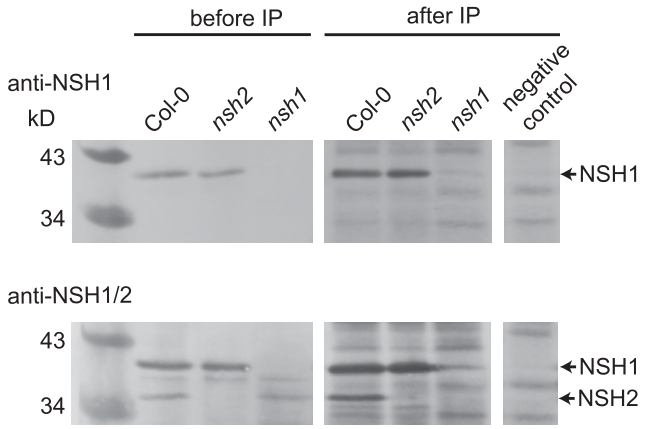

Figure 7. Interaction of Native NSH1 and NSH2 in Roots of Arabidopsis.

Root cell lysates of Col-0, *nsh1*, and *nsh2* were IPed with anti-NSH1 antibody. The presence of the nucleoside hydrolases in the clarified lysate (before IP) and after the IP was detected by immunoblot with anti-NSH1 (top) and dual-specific anti-NSH1/2 antibodies (bottom). The last lane in both panels is an IP control without added root extracts.

on nucleoside accumulation in that tissue (Figure 9). A small accumulation of xanthosine, but not of inosine or uridine, was observed in the *nsh2* background, again confirming the general involvement of NSH2 in xanthosine degradation, but not supporting the idea of an especially prominent role of NSH2 in roots. In the *NSH1* mutant, a strong accumulation of xanthosine and uridine and an increase in the inosine concentration were detected, re-emphasizing the central role of NSH1 for the catabolism of these nucleosides.

NSH1, NSH2, and the NSH1-NSH2 complex were purified after transient (co)expression in leaves of *N. benthamiana*, and the specific activities were assessed with 250 μM xanthosine, 250 μM inosine, and 250 μM uridine as substrates (Table 1). NSH1 was most active with uridine, approximately ninefold less active with xanthosine, and showed only very low activity with inosine when this substrate was offered at higher concentrations (Supplemental Table 1). NSH2 did not hydrolyze any of these substrates, irrespective of concentration. Interestingly, the NSH1-NSH2 complex showed a marked activity with xanthosine, much stronger than that of NSH1 alone, and also some activity with inosine and uridine. By determining the kinetic constants, it became clear that the catalytic efficiency (k_{cat}/K_m) of the NSH1-NSH2 complex for xanthosine is ~80-fold higher than the catalytic efficiency of NSH1 alone. This is due to a lower K_m and a higher k_{cat} (Table 2). For uridine, the situation is reversed: the catalytic efficiency of the NSH1-NSH2 complex is more than threefold lower than that of NSH1 alone, mainly due to a higher K_m of the complex. For inosine, we were unable to determine the kinetic constants of NSH1 with our spectrophotometric method, because the required substrate concentrations would have exceeded the measurable range, but Jung et al. (2009) determined a K_m value of 1.4 mM and a k_{cat} value of 8.7 s^{-1} using enzyme purified from *E. coli* and a radiometric assay. Hence, with a K_m value of 0.6 mM and a k_{cat} value of 42.3 s^{-1} for inosine, the catalytic efficiency of the NSH1-NSH2 complex is more than an order of magnitude higher than that of NSH1 alone. We conclude that the NSH1-NSH2 complex is a highly efficient xanthosine hydrolase that also has inosine as well as weaker uridine hydrolase activity. The xanthosine/inosine hydrolase activities exceed by far those of the NSH1 homodimer, which is the better uridine hydrolase.

We asked whether a xanthosine/inosine hydrolase activity of NSH2 is activated by the interaction with NSH1, or whether NSH2 is intrinsically inactive, but can boost the xanthosine/inosine hydrolase activity of NSH1. To address this question, active site mutants were generated by changing a catalytically essential Asp to Ala in NSH1 (D29A) and NSH2 (D14A) (Supplemental Figure 4). In the resulting mutants, called ΔNSH1 and ΔNSH2, nucleoside hydrolase activity was abrogated (Table 1; Supplemental Table 1). Interestingly, the ΔNSH1-NSH2 complex was highly active with xanthosine and retained low inosine hydrolase activity, demonstrating that NSH2 is an active xanthosine inosine nucleosidase, which requires the interaction with NSH1 for activation. The NSH1-ΔNSH2 complex also retained some hydrolytic activity for

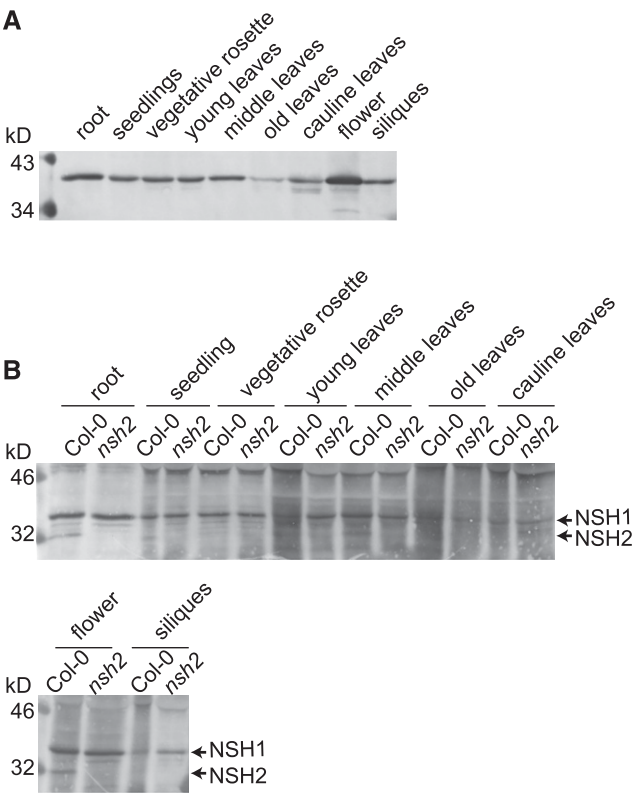

Figure 8. Protein Abundance of NSH1 and NSH2 in Different Tissues at Distinct Developmental Stages.

(A) Immunoblot developed with anti-NSH1 antibody. A 2:1 buffer-to-sample ratio was used for extraction, and 12 μL of sample were loaded per lane. Samples: 10-d-old seedlings grown on agar plates, roots and the rosette of a 4-week-old plant before bolting grown in soil, young leaves (leaves up to position 14), middle leaves (13 to 7), old leaves (6 to 1), cauline leaves, flowers, and siliques of a 6-week-old plant.

(B) As in **(A)** but developed with the dual-specific NSH1/2 antibody and using the *NSH2* mutant additionally to the wild type, as negative control for the NSH2 signal.

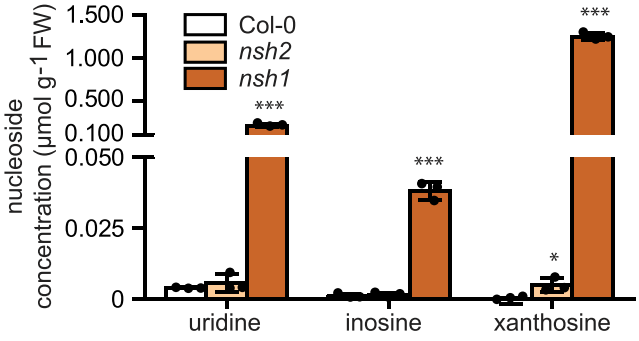

Figure 9. Nucleoside Concentration in Root Extracts of the Nucleoside Hydrolase Mutants and the Wild Type.

Uridine, inosine, and xanthosine concentrations in root extracts of hydroponically grown Col-0, *nsh2*, and *nsh1* plants. Individual data points (dots) of three biological replicates and the mean (bar) are shown. Error bars are SD. The asterisks indicate significant differences between the mutants and the wild type as determined by unpaired two-tailed *t* tests (*P < 0.05; ***P < 0.001). FW, fresh weight.

xanthosine and uridine, showing that both enzymes actively contribute to the enzymatic characteristics of the NSH1-NSH2 complex. Xanthosine- and inosine-specific activities are mainly contributed by NSH2, whereas uridine-specific activity appears to reside mainly in NSH1. Nonetheless, NSH1 alone is sufficiently active with xanthosine to prevent strong accumulation of this metabolite in planta (Figures 3, 4, and 9).

To assess whether the tagged variants of NSH1 and NSH2 are functional in vivo, the respective knockout lines were transformed with constructs encoding Strep- and myc-tagged variants of the enzymes. Additionally, the *NSH1* mutant was transformed with a construct encoding the Strep-tagged inactive ΔNSH1 (D29A) variant. According to our in vitro data, NSH2 might be activated by ΔNSH1 in this *nsh1* background, creating a situation where NSH2 is active but NSH1 is inactive. Using immunoblots, the expression of the proteins in the corresponding transgenic plants was shown (Figure 10A). In the respective lines, xanthosine, inosine, and uridine were quantified in seeds, 7-d-old seedlings, and rosettes of 4-week-old plants just before bolting (Figure 10B). Xanthosine accumulation in the *nsh2* background was suppressed by the *NSH2* transgenes, and xanthosine, inosine, and uridine accumulation in the *nsh1* background was suppressed by the *NSH1* transgenes, demonstrating that the myc- and Strep-tagged variants of these enzymes are functional in vivo. Interestingly, xanthosine and inosine accumulation in the *nsh1* background was also completely suppressed by the *ΔNSH1* transgene. Apparently, the activation of native NSH2 by this inactive ΔNSH1 variant is sufficient for the maintenance of the wild-type xanthosine and inosine homeostasis in seeds, seedlings, and rosettes. This demonstrates that NSH2 is an efficient xanthosine and inosine hydrolase in vivo and shows that NSH2 must be expressed in leaf tissue, although it was difficult to clearly detect it there with our dual-specific antibody (Figure 8B). In seeds, but not in seedlings and rosettes, even the high uridine concentration in the *nsh1* background was reduced by activation of NSH2 with ΔNSH1. At such an elevated substrate concentration as found in the *nsh1* seed, the weak uridine hydrolase activity of the ΔNSH1-NSH2 complex detected in vitro (Supplemental Table 1) seems to be sufficient to degrade some uridine over time.

Dark Stress–Induced Nucleotide Catabolism

Although NSH2 is a highly efficient xanthosine hydrolase, its abrogation only had a small influence on xanthosine concentrations in seeds, seedlings, rosettes, and roots (Figures 3, 4, 9, and 10). We wondered whether the impact of *NSH2* abrogation would increase in a situation where the flux through purine nucleoside catabolism is higher. Therefore, we exposed the 3-week-old wild-type and different *NSH* mutant plants to dark stress, known to boost nucleotide catabolism (Jung et al., 2011; Schroeder et al., 2018), and xanthosine, inosine, and uridine concentrations were determined after 2 and 3 d of exposure to darkness. In the wild type and in the *nsh2* background, the xanthosine concentration did not increase (Figure 11). By contrast, in the *nsh1* background, the xanthosine concentration was increased ~25-fold by the second day and by ~65-fold by day 3 to 22.8 µmol/g dry weight (DW). It appears that the requirement for NSH2 is not rising with higher flux through nucleoside catabolism. Interestingly, the massive dark-induced xanthosine accumulation in the *nsh1* background was prevented by the inactive ΔNSH1 transgene, showing that the activity of native NSH2, which is induced by ΔNSH1, is sufficient to hydrolyze xanthosine even in situations of high metabolic flux.

The inosine concentration was very low throughout the experiment and only rose by day 3 in the *nsh1* background to an ~65-fold lower concentration as found for xanthosine. However, the ~0.35 µmol/g DW reached at day 3 was the highest tissue concentration of inosine observed in any of our experiments. The lack of any inosine accumulation up to the second day strongly supports the idea that inosine is not an intermediate of AMP/IMP catabolism. The increase in inosine concentration on the third day

Table 2. Kinetic Constants of NSH1 and the NSH1-NSH2 Complex

Nucleoside	NSH1				NSH1-NSH2			
	K_m (mM)	k_{cat} (s^{-1})	k_{cat}/K_m (s^{-1} mM^{-1})	R^2	K_m (mM)	k_{cat} (s^{-1})	k_{cat}/K_m (s^{-1} mM^{-1})	R^2
Xanthosine	0.52	2.65	5.10	0.96	0.06	23.3	389.2	0.99
Inosine	—	—	—	—	0.60	42.3	70.5	0.90
Uridine	0.73	33.5	45.9	0.98	4.30	55.3	12.9	0.95

Dashes indicate that data were not determined.

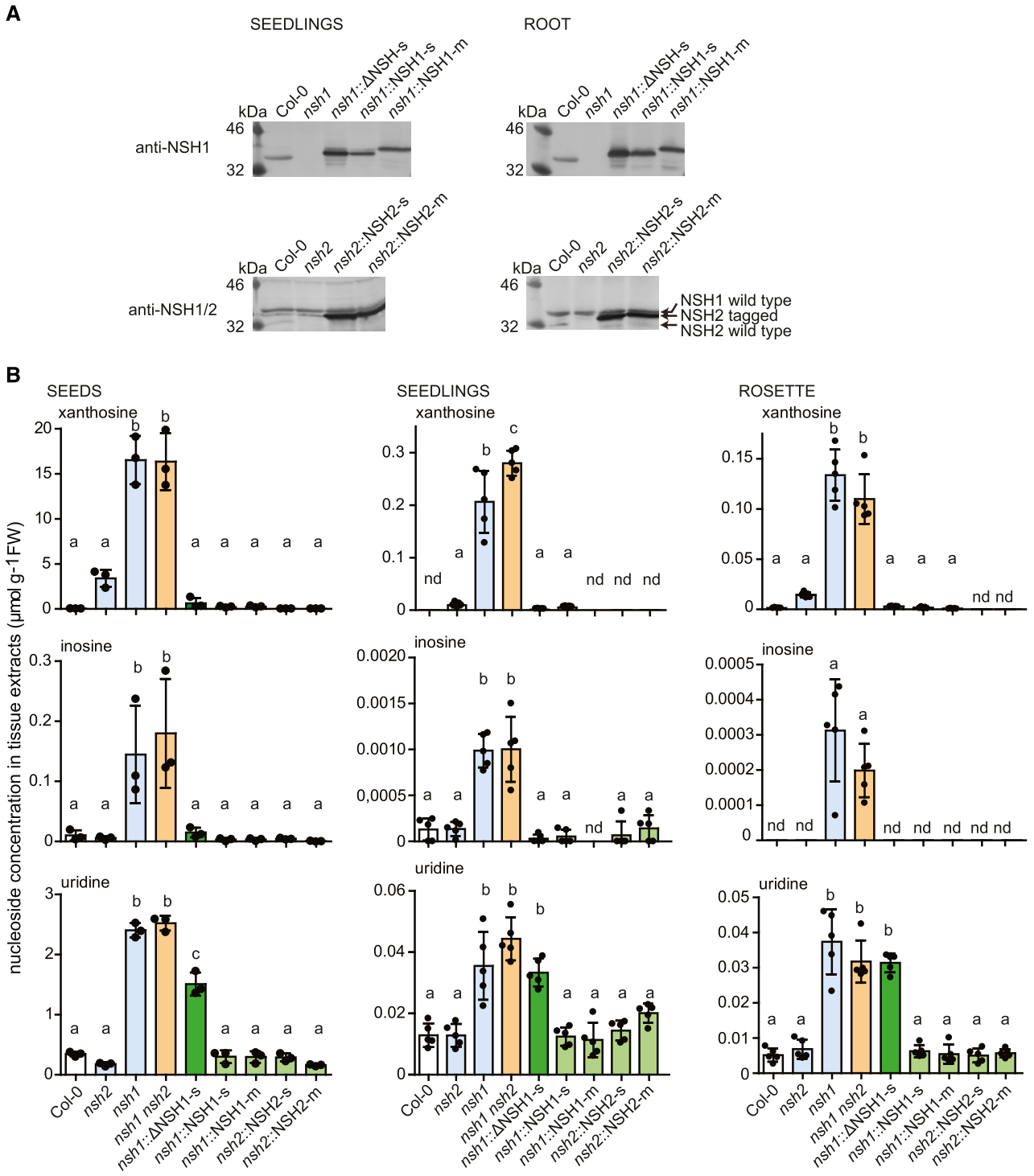

Figure 10. Protein Expression and Nucleoside Accumulation in Transgenic Lines Expressing Nucleoside Hydrolase Variants.

(A) Expression of Strep- or myc-tagged NSH1 (NSH1-s, NSH1-m) as well as an enzymatically inactive Strep-tagged NSH1 point mutant (ΔNSH1-s) in the *nsh1* background detected in seedlings and roots by immunoblots developed with the anti-NSH1 antibody (top panels). Expression of Strep- or myc-tagged NSH2 (NSH2-s, NSH2-m) in the *nsh2* background detected in seedlings and roots by immunoblots developed with the dual-specific anti-NSH1/2 antibody (bottom panels). Seven-day-old seedlings and roots from 4-week-old plants were used.

(B) Xanthosine, inosine, and uridine concentration in extracts from seeds, 7-d-old seedlings, and rosette leaves of 4-week-old plants of the wild type (white), the nucleoside hydrolase single mutants (blue), and the double mutant (orange) and the indicated transgenic lines overexpressing tagged variants of NSH1

in the *nsh1* background might be caused by the onset of autophagy-mediated vacuolar tRNA turnover by that time.

We repeated the dark stress experiment with the wild type and the *xdh*, *hgprt*, and *xdh hgprt* lines, quantifying xanthine and hypoxanthine (Figure 12A). Despite an already strongly elevated xanthine concentration in *xdh* plants at the beginning of the experiment, the xanthine concentration was further increased by dark stress, demonstrating that purine catabolism is operating, whereas the hypoxanthine concentration in the *xdh hgprt* line, which is blocked in catabolism and salvage, stayed constant. Again, these data strongly suggest that AMP/IMP is not catabolized via hypoxanthine.

One may argue that the permanently high xanthine concentration in the *xdh* background already disturbs purine catabolism. We therefore performed an additional short-term dark exposure experiment with the wild type and the *HGPRT* mutant, where we used allopurinol, which strongly inhibits XDH, causing an acute lack of XDH activity after treatment. Long-day-grown seedlings were optionally exposed at the end of the night to allopurinol and then either grown in a normal day or exposed to darkness for 8 h to stimulate purine nucleotide catabolism (Figure 12B). Allopurinol-treated plants accumulated xanthine, but this accumulation was approximately three times stronger in the dark (~55 nmol g^{-1}) than in the light (~17 nmol g^{-1}), demonstrating that purine nucleotide catabolism was more active under dark conditions. In the *hgprt* background, the allopurinol-treated plants also accumulated hypoxanthine, but slightly more in the light compared with darkness (~5 nmol g^{-1}). This is again consistent with the idea that hypoxanthine is not derived from AMP/IMP catabolism. It also confirms that hypoxanthine is usually processed by both XDH and HGPRT, because it only accumulates if both activities are compromised. As expected, the guanine concentration was higher in the *HGPRT* mutant than in the wild type, but the concentration did not change over time or by treatment in both genotypes, confirming that guanine is not an intermediate of purine nucleotide catabolism in Arabidopsis.

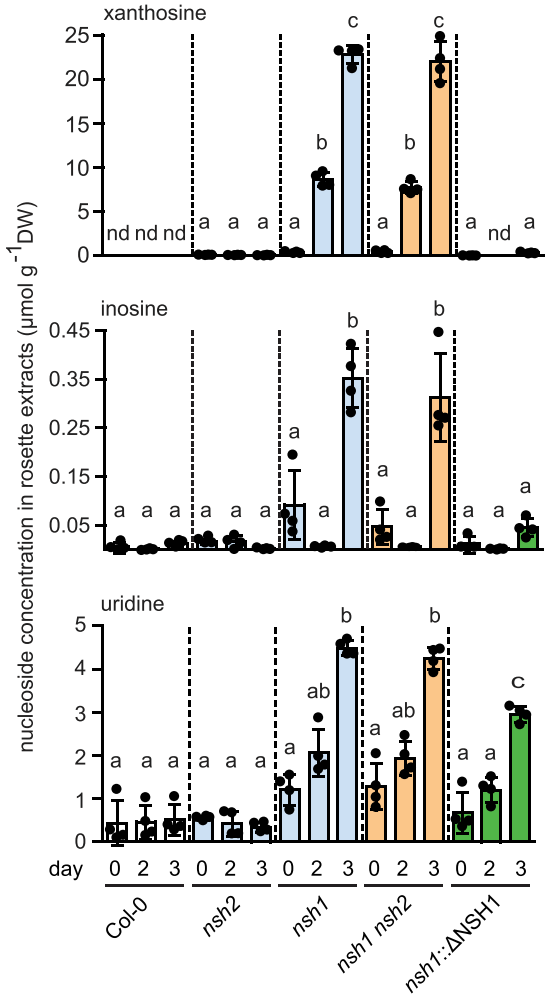

Figure 11. Alteration of Nucleoside Content in Nucleoside Hydrolase Variants during Dark Stress.

Xanthosine, inosine, and uridine were quantified in rosettes of 3-week-old plants before dark exposure (day 0) and after 2 and 3 d of darkness. Individual data points (dots) of four biological replicates and the mean (bar) are shown. Error bars are SD. The statistical analyses were performed using one-way ANOVA with Tukey's post test. Different letters indicate significant differences ($P < 0.05$). nd, not detectable. DW, dry weight.

DISCUSSION

When the data presented here are integrated with the current knowledge about purine nucleotide catabolism in vascular plants, a revised model can be drawn (Figure 13; Supplemental Figure 5). Central differences to the current model (Figure 1) are the absence of an IMPP reaction connecting IMP to inosine and hypoxanthine and the placement of NSH2 in complex with NSH1 on the metabolic map as xanthosine and inosine nucleoside hydrolase. Doubts about the existence of an IMPP in vivo have been raised earlier in work with soybean and cowpea, where purine nucleotide catabolism is highly active in nodules to generate the ureides allantoin and allantoate (Supplemental Figure 5) as export forms of fixed nitrogen. Shelp and Atkins (1983) concluded from work on cell-free extracts of cowpea nodules with labeled IMP that the production of ureides rather occurs via IMP oxidation than IMP dephosphorylation. In soybean nodules, only xanthine, but no hypoxanthine, was observed after allopurinol treatments (Fujihara and Yamaguchi, 1978; Boland and Schubert, 1982), which cannot be explained by preferential hypoxanthine salvage in this tissue, since the nodule is a site of strong purine nucleotide catabolism. A

Figure 10. (continued).

and NSH2 (green) as well as the inactive D29A point mutant of NSH1 (ΔNSH1, dark green) in the corresponding mutant backgrounds. Individual data points (dots) of biological replicates ($n = 5$ for seedlings and rosettes and $n = 3$ for seeds derived from different mother plants) and the mean (bar) are shown. Error bars are SD. The statistical analyses were performed using one-way ANOVA with Tukey's post test. Different letters indicate significant differences ($P < 0.05$). nd, not detectable. FW, fresh weight.

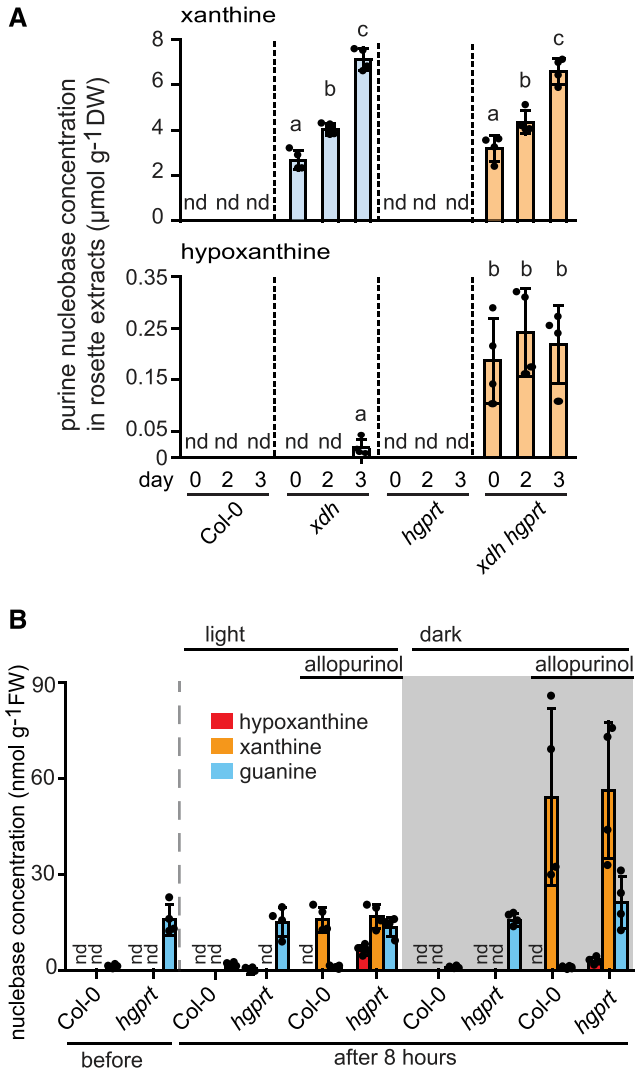

Figure 12. Changes in Nucleobase Concentrations during Long-Term and Short-Term Dark Stress.

(A) Xanthine and hypoxanthine were quantified in the wild type and the *XDH HGPRT* double mutant as well as the respective single mutants using rosettes of 3-week-old plants before dark exposure (day 0) and after 2 and 3 d of darkness. Individual data points (dots) of four biological replicates and the mean (bar) are shown. Error bars are SD. The statistical analyses were performed using one-way ANOVA with Tukey's post test. Different letters indicate significant differences ($P < 0.05$). nd, not detectable. DW, dry weight.

(B) Concentration of nucleobases in the 7-day-old wild-type and *hgprt* seedlings at the end of the night (before) and after 8 h in light or in darkness, when plants were optionally treated with allopurinol at the beginning of the 8-h period. Plants from four growth plates (half-strength MS medium) were analyzed per treatment. Individual data points (dots) of the biological replicates ($n = 4$ biological replicates) and the mean (bar) are shown. Error bars are SD. On each plate both genotypes were grown and treated in parallel. FW, fresh weight.

consequence of the absence of IMPP in Arabidopsis is that inosine and hypoxanthine are not intermediates of AMP/IMP catabolism and that both AMP and GMP are catabolized via xanthosine. Dahncke and Witte (2013) postulated that xanthosine is exclusively generated by GSDA in Arabidopsis, because xanthosine could not be detected in an *NSH1 GSDA* double mutant using HPLC coupled with UV detection. Here, we present several lines of evidence that xanthosine is not exclusively produced from guanosine deamination by GSDA but also from XMP dephosphorylation (Figure 4), which leads us to postulate that an as-yet unidentified XMPP must exist. In cell-free extracts of nodules from cowpea, ureide synthesis was supported significantly better by XMP than by GMP, and GMP was not generated from XMP (Atkins, 1981), indicating that an XMPP is active in this tissue. It is tempting to speculate that AMP is degraded to xanthosine via IMP and XMP using a XMPP and that GMP is catabolized by a GMP phosphatase and GSDA. However, our data consistently show that the *GSDA* mutant is a surprisingly strong suppressor for the accumulation of purine ring catabolites (Figures 2 to –4), suggesting that the route via the XMPP is less important in Arabidopsis. This might be correct, but one needs to bear in mind that the *GSDA* mutant accumulates high amounts of guanosine, which could potentially inhibit XMPP. In this scenario, a *GSDA* mutant would not only lack GSDA activity but also be partially compromised in XMPP activity. Because of these possible complications, the quantitative aspects of our data should not be overinterpreted.

One puzzling aspect of purine nucleotide catabolism according to the current model (Figure 1) is the parallel presence of catabolic and salvage steps in the same compartment and probably the same tissue. Most of the enzymes shown in Figure 1 are located in the cytosol. For the phosphatases, the location is unknown, whereas an IGK has been partially purified from a mitochondrial preparation in *Helianthus tuberosus* (Combes et al., 1989), indicating that this enzyme might reside in the mitochondria. Why would IMP and GMP first be degraded to hypoxanthine and guanine, respectively, and then salvaged back to IMP and GMP by HGPRT in a futile cycle? With the discovery of GSDA (Dahncke and Witte, 2013), it became clear that guanine is unlikely an important intermediate of G nucleotide catabolism in Arabidopsis. The data presented here suggest that only xanthine, but neither hypoxanthine nor guanine, is an intermediate of AMP and GMP catabolism. Therefore, in the revised model (Figure 13), HGPRT is completely decoupled from AMP and GMP catabolism. The enzyme salvages guanine, probably generated by spontaneous depurination of nucleotides and nucleic acids. It also salvages hypoxanthine, possibly derived from DNA and nucleotide pool maintenance as well as from vacuolar tRNA turnover releasing inosine, which is hydrolyzed by NSH1-NSH2 to hypoxanthine and ribose. Uptake of soilborne nucleosides from the rhizosphere for salvage or plant nitrogen nutrition is probably another source of inosine (Tokuhisa et al., 2010), possibly explaining why NSH enzymes are most strongly expressed in roots (Figure 8; Riegler et al., 2011). In agreement with pulse-chase studies using radiotracers, our data show that hypoxanthine is alternatively salvaged or degraded in vivo (Figures 3 and 12), although it is unclear which reaction prevails in undisturbed metabolism.

Another interesting complication in purine nucleotide metabolism is that the biosynthetic pathway for GMP and the catabolic

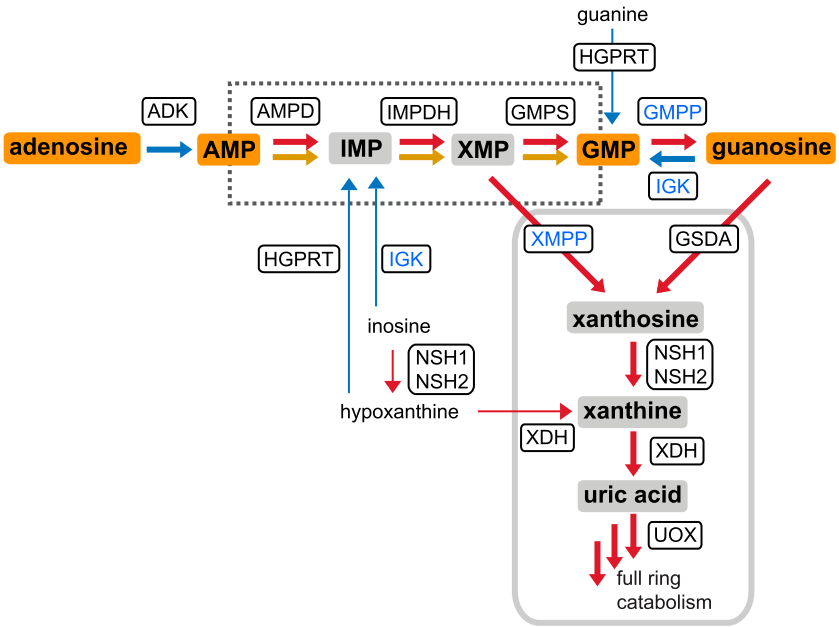

Figure 13. Updated Model of Purine Nucleotide Catabolism in Arabidopsis.

Metabolites with orange background are released in cytosolic (AMP, GMP) or vacuolar (adenosine, guanosine) RNA turnover. Blue, red, and yellow arrows indicate salvage, catabolic, and biosynthetic reactions, respectively. Note that reactions leading from AMP to GMP can be biosynthetic or catabolic depending on whether the degradation of AMP or the generation of GMP from AMP is dominating (dotted box). Metabolites within the box demarcated with a light gray line can only be catabolized and not salvaged. An extended version of the model is presented in Supplemental Figure 5. Enzymes: ADK, adenosine kinase; AMPD, AMP deaminase; IMPDH, IMP dehydrogenase; GMPS, GMP synthetase; HGPRT, hypoxanthine guanine phosphoribosyltransferase; XMPP, XMP phosphatase; GMPP, GMP phosphatase; IGK, inosine guanosine kinase; GSDA, guanosine deaminase; NSH1, nucleoside hydrolase 1; NSH2, nucleoside hydrolase 2; XDH, xanthine dehydrogenase; UOX, urate oxidase. Enzyme names are shown in blue if the corresponding enzyme is presumed to be involved but the genetic identity is unclear.

pathway for AMP share at least two common enzymes: AMP deaminase and IMP dehydrogenase. How biosynthetic versus catabolic fluxes are regulated is currently unclear, but a metabolic switch might reside on the XMPP and GMP synthetase enzymes, which both use XMP as substrate.

The genomes of plants encode two phylogenetically separated clades of cytosolic nucleoside hydrolases, NSH1 and NSH2 (Kopecná et al., 2013). An assignment of a functional role was relatively straightforward for NSH1 in Arabidopsis, because the corresponding mutant showed significant defects in the catabolism of xanthosine and uridine (Jung et al., 2009; Riegler et al., 2011) and inosine (Figure 3). By contrast, the functional role of NSH2 remained unresolved, although based on in vitro experiments, the enzyme appeared to be involved in xanthosine and inosine hydrolysis, and it was hypothesized that NSH2 might form a heterocomplex with NSH1 (Riegler et al., 2011). We show here that an *NSH1* mutant is actually a functional knockout of both NSH1 and NSH2, because NSH2 requires NSH1 for activity, but not vice versa. NSH2 was predicted to be a nucleosidase, which preferentially hydrolyzes xanthosine and inosine, because of two characteristic active site Tyr residues (Y233 and Y238) versus W247 and D252 in NSH1, which are indicative of an enzyme that prefers xanthosine and uridine (Kopecná et al., 2013). Nonetheless, the inosine concentration is not altered and the xanthosine concentration is only slightly elevated in the *nsh2* background, which could only be detected with our sensitive mass spectrometry method, but was not noted previously using less sensitive methods. Is NSH1 the more important enzyme and NSH2 only plays a minor role? One needs to look at a situation where NSH2 is the only active enzyme in vivo; this occurs in the *NSH1* mutant complemented with the inactive ΔNSH1 variant (Figures 10 and 11). Here, NSH2 alone can suppress xanthosine and inosine (but not uridine) accumulation normally observed in the *nsh1* background to the wild-type levels, for xanthosine consistently below the concentration found when only NSH1 is active (Figure 10B, *nsh2* background). Note that NSH2 is not overexpressed in this line and that its activation by the mutated ΔNSH1 might not be complete as indicated by our in vitro activity measurements (Table 1). The partial suppression of uric acid and xanthine accumulation in the *uox* and *xdh* background by *NSH2* mutation (Figures 2 and 3) demonstrates that flux through purine nucleotide catabolism is reduced in the absence of NSH2. We conclude that for xanthosine as well as inosine hydrolysis, NSH2 is at least as effective as NSH1 and that NSH2 is required for complete xanthosine homeostasis and undisturbed flux through purine nucleotide catabolism. It is possible that by modulation of NSH2 amounts, the hydrolytic capacity for distinct nucleosides could be steered, because the NSH1-NSH1 and NSH1-NSH2 complexes have clearly distinct enzymatic characteristics. It remains to be elucidated whether such a regulation actually occurs

and under which conditions a regulation of hydrolytic capacity for distinct nucleosides might be required.

METHODS

Cloning and Site-Directed Mutagenesis

The complementary DNAs (cDNAs) of *NSH1* and *NSH2* were amplified with the primer pairs 1905 + 1906 and 1904 + 1903, respectively (Supplemental Table 2), introducing *Nco*I and *Bam*HI restriction sites. For protein expression in *Nicotiana benthamiana* with N-terminal tags, the cDNAs were cloned into pXNS2pat-Strep (V42; Cao et al., 2010) and pXNS2pat-myc (V103), generated from V42 by replacing a *Xho*I *Sfo*I fragment with the annealed primers N0379 and N0380 encoding a myc tag. *NSH2* was further cloned via *Nco*I and *Bam*HI into pXNS2cpmv-Strep (V90). This vector was created by first cloning a 523-bp *Xho*I *Sal*I fragment from V69 (Myrach et al., 2017) into the *Xho*I site of V42 and then amplifying a 189-bp fragment from V69 with primers N0004 and N0005, cutting it with *Spe*I and *Xba*I, and cloning it via *Xba*I into the modified V42. The resulting vector V90 contains 5′ and 3′ untranslated region enhancer sequences of the *Cowpea mosaic virus* (CPMV) RNA-2, leading to enhanced protein expression (Figure 5A). The *NSH1* and *NSH2* cDNAs were also cloned into pET30nco-CTH (V48) (Myrach et al., 2017) via *Nco*I and *Sma*I for expression of the untagged proteins in *Escherichia coli*. The cDNAs of *NSH1* and *NSH2* were amplified with the primers 1905 + P106 and 1903 + P105respectively, to introduce a *Sma*I site and a STOP codon at the 3′ end.

Site-directed mutagenesis of *NSH1* was performed with the primer pairs P468 + P447 and P446 + P469 using the *NSH1* cloned in V42 as template. The two fragments were assembled with a NEBuilder HiFi DNA Assembly Cloning kit (New England Biolabs), and the resulting fragment was further amplified with P468 + P469 and cloned into V42 and V103 via *Nco*I and *Bam*HI. The same procedure was followed to mutate *NSH2*. The primer pairs used were 0001 + P514 and P513 + 0002.

Plant Material and Cultivation

The following T-DNA mutants of Arabidopsis (*Arabidopsis thaliana*) from the SALK collection (Alonso et al., 2003), the GABI-Kat collection (Kleinboelting et al., 2012), and the SAIL collection (Sessions et al., 2002) were used: SALK083120, *nsh1-1* (At2g36310; Jung et al., 2011); SALK128723, *nsh2-1* (At1g05620; Riegler et al., 2011); SAIL305B08, *gsda-1* and GK432D08, *gsda-2* (At5g28050; Dahncke and Witte, 2013); GK015E03, *hgprt-2* (At1g71750; Schroeder et al., 2018); GK049D04, *xdh1-2* (At4g34890; Hauck et al., 2014) allele assignment by Ma et al. (2016); and *uox-1* (Hauck et al., 2014) allele assignment here. The first mentioning and allele assignments in the literature are cited. The wild type was Col-0.

Double mutants were obtained by crossing *uox-1* and *xdh1-2*, *hgprt-2* and *uox-1*, *gsda-1* and *uox-1*, *gsda-2* and *uox-1*, *nsh2-1* and *uox-1*, *nsh1-1* and *uox-1*, *hgprt-2* and *xdh1-2*, *xdh1-2* and *gsda-2*, *xdh1-2* and *nsh2-1*, *xdh1-2* and *nsh1-1*, *gsda-2* and *nsh1-1*, and *nsh1-1* and *nsh2-1*. Triple mutants were obtained by crossing uox-1 nsh1-1 and uox-1 nsh2-1 and xdh1-2 nsh2-1 and xdh1-2 nsh1-1; the pollen donor is named last, respectively.

Complementation lines for *nsh1* were obtained by transforming constructs in the vectors V42 and V103 containing *NSH1* cDNAs under the control of the 35S promoter and leading to the expression of N-terminally Strep- or myc-tagged fusion proteins. For complementing *nsh2*, *NSH2* cDNAs cloned into the vectors V90 and V103 were used. A construct in V42 encoding the N-terminally Strep-tagged and mutated D29A version of NSH1 was also transformed into the *nsh1* background.

Arabidopsis and *N. benthamiana* were grown in a controlled growth chamber (at 16-h-light/8-h-dark cycle of 85 μmol m^{-2} s^{-1}, 22°C day, 18°C night, 60% RH). For metabolic profiling, plants were grown on full nutrient soil or on agar plates prepared with half-strength Murashige and Skoog (MS) media. *uox-1* and the double and triple mutants in the *uox-1* background were first germinated on plates supplemented with 1% (w/v) Suc and, after seedling establishment, transferred to soil (Hauck et al., 2014). For the allopurinol treatment, plates with 7-d-old seedlings were sprayed with 500 μL of a 200 μM allopurinol solution (Ma et al., 2016).

For the dark stress treatment, plants were grown as described by Schroeder et al. (2018). To harvest root material for the IP experiments, plants were grown hydroponically using an Araponics system (Araponics). Seeds were sown in half-strength MS media with 0.65% phytoagar and placed in the Araponic box filled with deionized water. One week after planting, the Araponic box was filled with nutrient solution formulated as described by Myrach et al. (2017) and renewed every 2 weeks. Plants were grown for 6 weeks in a growth chamber under short-day conditions (Binder 865 with Osram Lumilux lights, 8-h-light/16-h-dark cycle of 60 μmol m^{-2} s^{-1}, 20°C day, 18°C night, 60% RH).

Protein Purification and Determination of Kinetic Constants

The N-terminally Strep-tagged variants of NSH1 and NSH2 were affinity purified after transient expression in *N. benthamiana* as described by Werner et al. (2008), but adjusting optical densities (ODs) of the helper Agrobacteria carrying the p19 silencing inhibitor construct to 0.1 and all the other bacterial strains to 0.4. In copurification experiments where Strep- and myc-tagged variants of nucleosidases were coexpressed, the OD was adjusted to 0.2. For activity assays, the heterocomplex was always purified via a Strep-tagged NSH2 enzyme.

The NSH activity was assessed spectrophotometrically using a UV/VIS spectrophotometer (UV-2700; Shimadzu), according to Kopecná et al. (2013) and Parkin (1996). The activity assay was set up at room temperature, in a 0.5-cm quartz cuvette, in a total volume of 1 mL. The reaction buffer was 100 mM HEPES , pH 8, mixed with substrates at specific concentrations. The reaction was initiated by adding 5 to 10 μL of purified NSH1 or NSH2 and 10 to 30 μL of purified NSH1-NSH2 complex. The activity was determined by monitoring the absorption decrease due to the consumption of xanthosine ($\Delta\varepsilon_{248} = -3.7$ mM^{-1} cm^{-1}; Kopecná et al., 2013), uridine ($\Delta\varepsilon_{280} = -1.8$ mM^{-1} cm^{-1}; Kopecná et al., 2013), and inosine ($\Delta\varepsilon_{280} = -0.92$ mM^{-1} cm^{-1}; Parkin, 1996). The protein concentration was determined with a BSA standard curve resolved on an SDS-PAGE gel and stained by colloidal Coomassie Brilliant Blue R 250 (Roth). Band intensities were quantified with an Odyssey Fc Imager (LI-COR). The specific activities of the heterocomplexes were calculated normalizing the activity per milligram of NSH dimer. The kinetic constants were determined using the following concentrations: 0.1, 0.2, 0.4, 0.6, 1.0, and 1.6 mM for uridine; 0.03, 0.06, 0.12, 0.24, 0.30, and 0.45 mM for xanthosine; and 0.25, 0.5, 0.75, 1.0, 1.5, and 2.0 mM for inosine. The curves were recorded three times, and the kinetic parameters were determined by fitting the data to the Michaelis–Menten equation using Prism V4 software (GraphPad).

Electrophoresis and Immunoblotting

SDS gel electrophoresis, immunoblotting for the detection of the Strep-tagged proteins, and Coomassie Brilliant Bl Brilliant Blue R 250 staining were performed as described by Witte et al. (2004). Myc-tagged proteins were detected using a mouse anti–c-myc antibody (catalog no. 11667149001; lot no. 18302300; dilution, 1:400; Roche) and a goat anti-mouse IgG alkaline phosphatase–conjugated secondary antibody (catalog no. A3562; lot no. SLBT8638; dilution, 1:10,000; Sigma-Aldrich). The native NSH1 and NSH2 from Arabidopsis were detected with a rabbit anti-NSH1 antibody (0.2 μg mL^{-1}) and anti-NSH1/2 dual-specific antibody (1 μg mL^{-1}). As secondary antibody, a goat anti-rabbit IgG alkaline phosphatase conjugate (catalog no. A3687; lot no. SLBC3108; dilution, 1:30,000; Sigma-Aldrich) was used.

For the detection of NSH1 and NSH2 in different tissues, the tissues were ground with 2 volumes of protein extraction buffer (100 mM Hepes, pH 8,5 mM EDTA, 15 mM DTT, 100 mM NaCl, and 0.5% [v/v] Triton X-100) and centrifuged at 20,000*g* at 4°C for 10 min. Samples (12 μL) were loaded on a 10% SDS polyacrylamide gel. The rosette and the root correspond to the entire rosette and root of 4-week-old plants before bolting. The 6-week-old flowering plants were separated into the different tissues according to Schroeder et al. (2018).

Generation of Polyclonal Antisera and Antibody Production

Untagged NSH1 and NSH2 were expressed in *E. coli* BL21 from cDNAs cloned in vector pET30nco-CTH (V48). Cells were grown in 1.5 liters of Luria-Bertani medium and induced by isopropyl-β-D-thiogalactoside after reaching an OD of 0.5. After 3 h of induction, cells were harvested, the pellet was resuspended in 80 mL of lysis buffer (50 mM Tris-HCl, pH 8.0, 0.25% [w/v] Suc, and 1 mM EDTA, pH 8.0) and vortexed. Then, 200 mg of lysozyme were added in 20 mL of lysis buffer, and the slurry was incubated on ice for 30 min. Cells were disrupted by sonication on ice, and 200 mL of detergent buffer (20 mM Tris-HCl, pH 7.5, 2 mM EDTA, pH 8.0, 200 mM NaCl, 1% [w/v] deoxycholic acid, and 1% [v/v] Nonidet P-40) was added. The lysate was centrifuged at 5000*g* for 10 min, the supernatant was removed, and the pellet was resuspended in 250 mL of washing buffer (0.5% [v/v] Triton X-100 and 1 mM EDTA, pH 8.0). Centrifugation and resuspension were repeated until a tight pellet was obtained. The pellet was washed in 250 mL of 70% ethanol [v/v], suspended in a small volume of freshly prepared PBS, and used for commercial rabbit antisera production and antibody purification (immunoGlobe).

The initial antibodies against NSH1 and NSH2 showed cross-reactivity for both NSH proteins. Therefore, the anti-NSH1 antiserum was run eight times over a column with immobilized NSH2 to deplete the serum from the anti-NSH2 cross-reacting antibody. The flow-through was then passed over a column with immobilized NSH1, and the eluted fraction represents the specific anti-NSH1 antibody. The dual anti-NSH1/2 was purified from the anti-NSH2 antiserum by running it once over a column with immobilized anti-NSH2, and the eluted fraction was used as antibody.

Immunoprecipitation

IP was performed using the Pierce Classic IP kit using the anti-NSH1 antibody (2 μg). Roots (300 mg) from 6-week-old Arabidopsis plants grown hydroponically in short-day conditions were ground in 540 μL of IP lysis/wash buffer (0.025 M Tris, 0.15 M NaCl, 0.001 M EDTA, 1% [v/v] Nonidet P-40, and 5% [v/v] glycerol, pH 7.4; Pierce Classic IP kit) and 60 μL of protease inhibitor (Complete, EDTA-free, protease inhibitor cocktail; Roche). The cell lysate was clarified at 20,000*g* for 10 min at 4°C and then treated according to the manufacturer's instructions.

Liquid Chromatography-Mass Spectrometry Analysis

Metabolite analysis was performed using an Agilent HPLC 1200 system coupled to an Agilent 6460C series triple quadrupole mass spectrometer. Nucleosides, nucleobases, and uric acid were separated by a Polaris 5 C18A column (50 × 4.6 mm; particle size, 5 μm; Agilent). Solvent A was 10 mM ammonium acetate, pH 9.5, to detect (and extract) uric acid and pH 7.5 to detect (and extract) nucleosides and nucleobases. Solvent B was methanol. The flow rate was 0.8 mL min^{-1} with the following gradient: 0 min, 5% B; 1.5 min, 5% B; 3.5 min, 15% B; 6 min, 100% B; 7 min, 100% B; 7.1 min, 5% B; and 13 min, 5% B. The injection volume was 20 μL. Uric acid was detected in negative mode; purine nucleosides, nucleobases, and uridine were detected in positive mode.

The extraction method from Hauck and Witte (2015) was used and adapted for metabolite extraction. For an efficient disruption of seed tissues, 10 mg of seeds, one 7-mm steel bead, and four 5-mm steel beads were placed in a 2-mL centrifuge vial, frozen in liquid nitrogen, and ground with a mixer mill MM 400 (Retsch) at a frequency of 19 Hz for 4 min 30 s. The sample holders were precooled in liquid nitrogen. Extraction buffer (mobile phase A, 500 μL) was added containing the internal standards (ISTDs) ^{15}N5-guanosine, ^{15}N2-uridine, and ^{15}N4-inosine (Cambridge Isotope Laboratories). Samples were immediately incubated at 95°C for 10 min and then centrifuged at 50,000*g* for 20 min. To remove any particles, the clarified samples were passed through a micro-spin filter (polyvinylidene difluoride, 0.2 μm; Thermo Fisher Scientific). Before loading, samples were generally diluted 10 times with extraction buffer without ISTDs; for measurement of uric acid, samples were diluted 100 times. For seedlings and roots, 50 mg of fresh material was used and treated in the same way except that grinding was performed with four 5-mm steel beads at 30 Hz. Seedling samples were diluted five times and root samples two times before loading. Rosettes of 4-week-old plants were harvested and frozen at −80°C. The tissue was freeze-dried, and 10 mg of material was extracted as described before, except that 1 mL of extraction buffer was used and the samples were diluted 10 times before measuring.

Guanosine, uridine, and inosine were quantified using the respective ISTD, and all other compounds were quantified by external standards (calibration curve). For external standards, standard solutions of xanthosine (0, 0.03, 0.06, 0.1, 0.5, 1, and 5 μg mL^{-1}), xanthine (0, 0.03, 0.06, 0.1, 0.5, 1, and 5 μg mL^{-1}), hypoxanthine (0, 0.01, 0.03, 0.06, 0.1, 0.5, and 1 μg mL^{-1}), and guanine (0, 0.01, 0.03, 0.06, 0.1, 0.5, and 1 μg mL^{-1}) or uric acid (0, 0.01, 0.05, 0.075, 0.1, 0.25, and 0.5 μg mL^{-1}) were added to the matrix (Col-0 extracts). Guanosine, uridine, xanthosine, xanthine, and guanine were analyzed using the method parameters described by Schroeder et al. (2018). Method parameters for inosine, hypoxanthine, and uric acid are listed in Supplemental Table 3. A signal-to-noise ratio < 10 was considered as not detectable (nd).

Statistical Analysis

All data were analyzed with Prism 8 software. One-way analysis of variance (ANOVA) with Tukey's post test was used. Different letters represent differences at a significance level of $P < 0.05$. Statistical analyses results are shown in Supplemental Data Set.

Accession Numbers

Sequence data from this article can be found in the GenBank/EMBL data libraries under the following accession numbers: *NSH1* (At2g36310), *NSH2* (At1g05620), *HGPRT* (At1g71750), *GSDA* (At5g28050), *XDH* (At4g34890), and *UOX* (At2g26230).

Supplemental Data

Supplemental Figure 1. Genetic suppression of seed germination and seedling establishment phenotypes of the urate oxidase mutant.

Supplemental Figure 2. Xanthine and guanosine content in rosettes of the *XDH GSDA* double mutant and the respective single mutants as well as the wild type.

Supplemental Figure 3. Calibration of the anti-NSH1/2 antibody and absolute quantification of NSH1 and NSH2 in roots.

Supplemental Figure 4. Position and function of the Asp mutated to Ala in NSH1 and NSH2.

Supplemental Figure 5. Extended updated model of purine nucleotide catabolism in Arabidopsis.

Supplemental Table 1. Specific activities of nucleoside hydrolases at elevated substrate concentrations for inosine and uridine.

Supplemental Table 2. Primers.

Supplemental Table 3. Method parameters for the LC-MS.

Supplemental Data Set. Statistical analyses results.

ACKNOWLEDGMENTS

We thank André Specht and Hildegard Thölke for technical support, Anting Zhu for generating pXNS2cpmv-Strep (V90), Nieves Medina Escobar for generating pXNS2pat-myc (V103), and Lennart Doering for performing the site-directed mutagenesis of *NSH1* and *NSH2*. We also thank Marc Heins, Sebastian Hoffmann, Sue Genschmer, Manuel Maidorn, Robin Meier, Vincenzo Puggioni, Jana Scharnberg, Anne Taraschewski, and Anting Zhu for generating and screening the double and triple Arabidopsis mutants used in this study. This work was financially supported by the Deutsche Forschungsgemeinschaft (grants WI3411/2-1 and WI3411/4-1) and the German Academic Exchange Service (DAAD full PhD fellowship to C.B.).

AUTHOR CONTRIBUTIONS

C.-P.W. conceived and designed this research. C.B. designed and performed the experiments and analyzed the data. C.-P.W. wrote the paper with the assistance of C.B.

Received November 26, 2018; revised January 28, 2019; accepted February 14, 2019; published February 20, 2019.

REFERENCES

Alonso, J.M., et al. (2003). Genome-wide insertional mutagenesis of *Arabidopsis thaliana*. Science **301:** 653–657.

Alseth, I., Dalhus, B., and Bjørås, M. (2014). Inosine in DNA and RNA. Curr. Opin. Genet. Dev. **26:** 116–123.

An, R., Jia, Y., Wan, B., Zhang, Y., Dong, P., Li, J., and Liang, X. (2014). Non-enzymatic depurination of nucleic acids: Factors and mechanisms. PLoS One **9:** e115950.

Ashihara, H., Takasawa, Y., and Suzuki, T. (1997). Metabolic fate of guanosine in higher plants. Physiol. Plant. **100:** 909–916.

Ashihara, H., Stasolla, C., Fujimura, T., and Crozier, A. (2018). Purine salvage in plants. Phytochemistry **147:** 89–124.

Atkins, C.A. (1981). Metabolism of purine nucleotides to form ureides in nitrogen-fixing nodules of cowpea (*Vigna unguiculata* L. Walp.). FEBS Lett. **125:** 89–93.

Atkins, C.A., Sanford, P.J., Storer, P.J., and Pate, J.S. (1988). Inhibition of nodule functioning in cowpea by a xanthine oxidoreductase inhibitor, allopurinol. Plant Physiol. **88:** 1229–1234.

Atkins, C.A., Storer, P.J., and Shelp, B.J. (1989). Purification and properties of purine nucleosidase from N_2- fixing nodules of cowpea (*Vigna unguiculata*). J. Plant Physiol. **134:** 447–452.

Bernard, C., Traub, M., Kunz, H.H., Hach, S., Trentmann, O., and Möhlmann, T. (2011). Equilibrative nucleoside transporter 1 (ENT1) is critical for pollen germination and vegetative growth in Arabidopsis. J. Exp. Bot. **62:** 4627–4637.

Boland, M.J., and Schubert, K.R. (1982). Purine biosynthesis and catabolism in soybean root nodules: Incorporation of 14C from 14CO2 into xanthine. Arch. Biochem. Biophys. **213:** 486–491.

Brychkova, G., Fluhr, R., and Sagi, M. (2008). Formation of xanthine and the use of purine metabolites as a nitrogen source in Arabidopsis plants. Plant Signal. Behav. **3:** 999–1001.

Cao, F.-Q., Werner, A.K., Dahncke, K., Romeis, T., Liu, L.-H., and Witte, C.-P. (2010). Identification and characterization of proteins involved in rice urea and arginine catabolism. Plant Physiol. **154:** 98–108.

Combes, A., Lafleuriel, J., and Lefloch, F. (1989). The inosine-guanosine kinase-activity of mitochondria in tubers of Jerusalem artichoke. Plant Physiol. Biochem. **27:** 729–736.

Dahncke, K., and Witte, C.-P. (2013). Plant purine nucleoside catabolism employs a guanosine deaminase required for the generation of xanthosine in Arabidopsis. Plant Cell **25:** 4101–4109.

Deng, W.W., and Ashihara, H. (2010). Profiles of purine metabolism in leaves and roots of *Camellia sinensis* seedlings. Plant Cell Physiol. **51:** 2105–2118.

Fernández, J.R., Byrne, B., and Firestein, B.L. (2009). Phylogenetic analysis and molecular evolution of guanine deaminases: From guanine to dendrites. J. Mol. Evol. **68:** 227–235.

Fujihara, S., and Yamaguchi, M. (1978). Effects of allopurinol [4-hydroxypyrazolo(3,4-d)pyrimidine] on the metabolism of allantoin in soybean plants. Plant Physiol. **62:** 134–138.

Hauck, O., and Witte, C.-P. (2015). Quantification of uric acid or xanthine in plant samples. Bio protoc. **5:** e1523.

Hauck, O.K., Scharnberg, J., Escobar, N.M., Wanner, G., Giavalisco, P., and Witte, C.-P. (2014). Uric acid accumulation in an Arabidopsis urate oxidase mutant impairs seedling establishment by blocking peroxisome maintenance. Plant Cell **26:** 3090–3100.

Jung, B., Flörchinger, M., Kunz, H.H., Traub, M., Wartenberg, R., Jeblick, W., Neuhaus, H.E., and Möhlmann, T. (2009). Uridine-ribohydrolase is a key regulator in the uridine degradation pathway of Arabidopsis. Plant Cell **21:** 876–891.

Jung, B., Hoffmann, C., and Möhlmann, T. (2011). Arabidopsis nucleoside hydrolases involved in intracellular and extracellular degradation of purines. Plant J. **65:** 703–711.

Katahira, R., and Ashihara, H. (2006). Dual function of pyrimidine metabolism in potato (*Solanum tuberosum*) plants: Pyrimidine salvage and supply of beta-alanine to pantothenic acid synthesis. Physiol. Plant. **127:** 38–43.

Kleinboelting, N., Huep, G., Kloetgen, A., Viehoever, P., and Weisshaar, B. (2012). GABI-Kat SimpleSearch: New features of the *Arabidopsis thaliana* T-DNA mutant database. Nucleic Acids Res. **40:** D1211–D1215.

Kopecná, M., Blaschke, H., Kopecny, D., Vigouroux, A., Koncitíková, R., Novák, O., Kotland, O., Strnad, M., Moréra, S., and von Schwartzenberg, K. (2013). Structure and function of nucleoside hydrolases from *Physcomitrella patens* and maize catalyzing the hydrolysis of purine, pyrimidine, and cytokinin ribosides. Plant Physiol. **163:** 1568–1583.

Lamberto, I., Percudani, R., Gatti, R., Folli, C., and Petrucco, S. (2010). Conserved alternative splicing of Arabidopsis transthyretin-like determines protein localization and S-allantoin synthesis in peroxisomes. Plant Cell **22:** 1564–1574.

Liu, X., Qian, W., Liu, X., Qin, H., and Wang, D. (2007). Molecular and functional analysis of hypoxanthine-guanine phosphoribosyltransferase from *Arabidopsis thaliana*. New Phytol. **175:** 448–461.

Ma, X., et al. (2016). Dual and opposing roles of xanthine dehydrogenase in defense-associated reactive oxygen species metabolism in Arabidopsis. Plant Cell **28:** 1108–1126.

Montalbini, P., and DellaTorre, G. (1995). Allopurinol metabolites and xanthine accumulation in allopurinol-treated tobacco. J. Plant Physiol. **147:** 321–327.

Myrach, T., Zhu, A., and Witte, C.-P. (2017). The assembly of the plant urease activation complex and the essential role of the urease accessory protein G (UreG) in delivery of nickel to urease. J. Biol. Chem. **292:** 14556–14565.

Parkin, D.W. (1996). Purine-specific nucleoside N-ribohydrolase from *Trypanosoma brucei brucei*. Purification, specificity, and kinetic mechanism. J. Biol. Chem. **271:** 21713–21719.

Pessoa, J., Sárkány, Z., Ferreira-da-Silva, F., Martins, S., Almeida, M.R., Li, J., and Damas, A.M. (2010). Functional characterization of *Arabidopsis thaliana* transthyretin-like protein. BMC Plant Biol. **10:** 30.

Riegler, H., Geserick, C., and Zrenner, R. (2011). *Arabidopsis thaliana* nucleosidase mutants provide new insights into nucleoside degradation. New Phytol. **191:** 349–359.

Schroeder, R.Y., Zhu, A., Eubel, H., Dahncke, K., and Witte, C.-P. (2018). The ribokinases of *Arabidopsis thaliana* and *Saccharomyces cerevisiae* are required for ribose recycling from nucleotide catabolism, which in plants is not essential to survive prolonged dark stress. New Phytol. **217:** 233–244.

Schubert, K.R., and Boland, M.J. (1990). The ureides. *In* The Biochemistry of Plants, BJ Miflin, and PJ Lea, eds, Academic Press, San Diego, pp. 197–283.

Serventi, F., Ramazzina, I., Lamberto, I., Puggioni, V., Gatti, R., and Percudani, R. (2010). Chemical basis of nitrogen recovery through the ureide pathway: Formation and hydrolysis of S-ureidoglycine in plants and bacteria. ACS Chem. Biol. **5:** 203–214.

Sessions, A., et al. (2002). A high-throughput Arabidopsis reverse genetics system. Plant Cell **14:** 2985–2994.

Shelp, B.J., and Atkins, C.A. (1983). Role of inosine monophosphate oxidoreductase in the formation of ureides in nitrogen-fixing nodules of cowpea (*Vigna unguiculata* L. Walp.). Plant Physiol. **72:** 1029–1034.

Stasolla, C., Katahira, R., Thorpe, T.A., and Ashihara, H. (2003). Purine and pyrimidine nucleotide metabolism in higher plants. J. Plant Physiol. **160:** 1271–1295.

Todd, C.D., and Polacco, J.C. (2006). AtAAH encodes a protein with allantoate amidohydrolase activity from *Arabidopsis thaliana*. Planta **223:** 1108–1113.

Tokuhisa, D., Shinano, T., Watanabe, T., Yamamura, T., and Osaki, M. (2010). Promotion of root growth by the application of inosine. Soil Science and Plant Nutrition **56:** 272–280.

Triplett, E.W., Blevins, D.G., and Randall, D.D. (1980). Allantoic acid synthesis in soybean root nodule cytosol via xanthine dehydrogenase. Plant Physiol. **65:** 1203–1206.

Werner, A.K., and Witte, C.P. (2011). The biochemistry of nitrogen mobilization: Purine ring catabolism. Trends Plant Sci. **16:** 381–387.

Werner, A.K., Sparkes, I.A., Romeis, T., and Witte, C.P. (2008). Identification, biochemical characterization, and subcellular localization of allantoate amidohydrolases from Arabidopsis and soybean. Plant Physiol. **146:** 418–430.

Werner, A.K., Romeis, T., and Witte, C.P. (2010). Ureide catabolism in *Arabidopsis thaliana* and *Escherichia coli*. Nat. Chem. Biol. **6:** 19–21.

Werner, A.K., Medina-Escobar, N., Zulawski, M., Sparkes, I.A., Cao, F.-Q., and Witte, C.-P. (2013). The ureide-degrading reactions of purine ring catabolism employ three amidohydrolases and one aminohydrolase in Arabidopsis, soybean, and rice. Plant Physiol. **163:** 672–681.

Witte, C.P., Noël, L.D., Gielbert, J., Parker, J.E., and Romeis, T. (2004). Rapid one-step protein purification from plant material using the eight-amino acid StrepII epitope. Plant Mol. Biol. **55:** 135–147.

Yin, Y., Katahira, R., and Ashihara, H. (2014). Metabolism of purine nucleosides and bases in suspension-cultured *Arabidopsis thaliana* cells. Eur. Chem. Bull. **3:** 925–934.

Zhou, W., Karcher, D., and Bock, R. (2014). Identification of enzymes for adenosine-to-inosine editing and discovery of cytidine-to-uridine editing in nucleus-encoded transfer RNAs of Arabidopsis. Plant Physiol. **166:** 1985–1997.

Zrenner, R., Stitt, M., Sonnewald, U., and Boldt, R. (2006). Pyrimidine and purine biosynthesis and degradation in plants. Annu. Rev. Plant Biol. **57:** 805–836.

Zrenner, R., Riegler, H., Marquard, C.R., Lange, P.R., Geserick, C., Bartosz, C.E., Chen, C.T., and Slocum, R.D. (2009). A functional analysis of the pyrimidine catabolic pathway in Arabidopsis. New Phytol. **183:** 117–132.